European Journal of Medicinal Chemistry 107 (2016) 119–132

Contents lists available at ScienceDirect

European Journal of Medicinal Chemistry

journal homepage: http://www.elsevier.com/locate/ejmech

Research paper

Potent and selective *N*-(4-sulfamoylphenyl)thiourea-based GPR55 agonists

Sari Yrjölä [a, *], Teija Parkkari [a, b], Dina Navia-Paldanius [b], Tuomo Laitinen [a], Agnieszka A. Kaczor [a, c], Tarja Kokkola [a], Frank Adusei-Mensah [a], Juha R. Savinainen [b], Jarmo T. Laitinen [b], Antti Poso [a, d], Amy Alexander [e], June Penman [e], Lisa Stott [e], Marie Anskat [e], Andrew J. Irving [e, f], Tapio J. Nevalainen [a]

[a] School of Pharmacy, Faculty of Health Sciences, University of Eastern Finland, PO Box 1627, FI-70211 Kuopio, Finland
[b] Institute of Biomedicine, School of Medicine, Faculty of Health Sciences, University of Eastern Finland, PO Box 1627, FI-70211 Kuopio, Finland
[c] Department of Synthesis and Chemical Technology of Pharmaceutical Substances with Computer Modeling Lab, Faculty of Pharmacy with Division of Medical Analytics, Medical University of Lublin, 4A Chodzki St., PL-20093 Lublin, Poland
[d] Division of Translational Gastrointestinal Oncology, Dept. of Internal Medicine I, University Hospital Tübingen, Otfried-Mueller-Strasse 10, 72076 Tübingen, Germany
[e] Division of Neuroscience, Medical Research Institute, Ninewells Hospital, University of Dundee, Dundee DD1 9SY, UK
[f] School of Biomolecular and Biomedical Science, University College Dublin, Belfield, Dublin D4, Ireland

ARTICLE INFO

Article history:
Received 22 April 2015
Received in revised form
15 October 2015
Accepted 28 October 2015
Available online 2 November 2015

Keywords:
G protein-coupled receptor 55
Molecular modeling
Structure–activity relationships

ABSTRACT

To date, many known G protein-coupled receptor 55 (GPR55) ligands are those identified among the cannabinoids. In order to further study the function of GPR55, new potent and selective ligands are needed. In this study, we utilized the screening results from PubChem bioassay AID 1961 which reports the results of Image-based HTS for Selective Agonists of GPR55. Three compounds, CID1792579, CID1252842 and CID1011163, were further evaluated and used as a starting point to create a series of nanomolar potency GPR55 agonists with *N*-(4-sulfamoylphenyl)thiourea scaffold. The GPR55 activity of the compounds were screened by using a commercial β-arrestin PathHunter assay and the potential compounds were further evaluated by using a recombinant HEK cell line exhibiting GPR55-mediated effects on calcium signalling. The designed compounds were not active when tested against various endocannabinoid targets (CB1R, CB2R, FAAH, MGL, ABHD6 and ABHD12), indicating compounds' selectivity for the GPR55. Finally, structure–activity relationships of these compounds were explored.

1. Introduction

G protein-coupled receptor 55 (GPR55) has emerged as an interesting novel target for a subset of cannabinoid ligands [1]. However, there are several features of GPR55 which do not support its classification as a cannabinoid receptor. Firstly, the strongest candidate for an endogenous GPR55 ligand is the non-cannabinoid lipid-mediator L-α-lysophosphatidylinositol (LPI), and especially its arachidonic acid derivate [2,3]. Secondly, results concerning the activation of GPR55 by cannabinoids have been controversial, with little consensus between groups [1]. Thirdly, it has even been suggested that GPR55 could act as an "anti-cannabinoid" receptor because GPR55 and cannabinoid receptor type 1 (CB1R) exhibit opposite roles in some systems, for example SR141716A is an inverse agonist/antagonist of the CB1R and an agonist at GPR55 [4,5]. Functional selectivity may also add to the complexity, where GPR55's pharmacology and downstream signalling vary in ligand- and system-dependent manners [1,6].

Despite the open questions related to GPR55 pharmacology, the receptor has been shown to have a role in an increasing array of physiological and pathological processes, including inflammation

Abbreviations: ABHD6/12, α/β-hydrolase domain containing 6/12; 2-AG, 2-arachidonoylglycerol; AEA, *N*-arachidonoylethanolamine; ARA-LPI, 1-arachidonoyl-2-hydroxy-*sn*-glycero-3-phosphoinositol; CB1/2R, cannabinoid receptor 1/2; CoMFA, comparative molecular field analysis; EA, ethyl acetate; EC, extra cellular; GlyT1, glycine transporter subtype 1; GPR55, G protein-coupled receptor 55; LPI, lysophosphatidylinositol; MGL, monoacylglycerol lipase; TMH, transmembrane helix.

* Corresponding author.
E-mail address: sari.yrjola@uef.fi (S. Yrjölä).

http://dx.doi.org/10.1016/j.ejmech.2015.10.050
0223-5234/

and pain [7–9], synaptic transmission [10], bone development [11], cancer [12–15], and gastrointestinal functions [16]. The GPR55/LPI system may also be associated with obesity in humans [17] whereas functional polymorphism in the GPR55 gene has been linked with anorexia nervosa [18].

To date, only a small set of selective GPR55 ligands have been reported in the literature because many ligands have been identified among the cannabinoids. In addition, even LPI has been shown to interact with certain plasma membrane ion channels and possibly additional GPCRs [19]. More selective and potent synthetic GPR55 ligands are thus needed as research tools to further study the pharmacology and function of this receptor.

Some new scaffolds for GPR55 agonists have been found by a high-content, high-throughput β-arrestin screen of 290,000 compounds (PubChem AID 1961) [20,21]. The study highlighted three new scaffolds represented by the compounds: ML184 (PubChem Compound ID: CID2440433), ML185 (CID1374043) and ML186 (CID15945391). The EC_{50} values for the compounds at GPR55 were reported to be 263 nM, 658 nM and 305 nM, respectively. The compounds were also demonstrated to be selective over CB1R, CB2R and GPR35. Three agonists found in the above mentioned screen, CID1792197, CID1172084 (analog of ML185) and ML184, have been used to identify the GPR55 agonist binding site by computational modeling [22]. Structurally similar compounds to ML184 have also been found in a diversity screening study conducted by GlaxoSmithKline [23]. However, the compounds have both GPR55 agonist and glycine transporter subtype 1 (GlyT1) inhibitor activity. The most potent GPR55 agonists of the study were GSK494581A (IC_{50} = 20 nM for GlyT1 and EC_{50} = 316 nM for GPR55) and GSK575594A (IC_{50} = 10 μM for GlyT1 and EC_{50} = 158 nM for GPR55) [23]. The structures of the above mentioned GPR55 agonists are shown in Fig. 1.

Only a few selective GPR55 receptor antagonists have been recently discovered. These include CID16020046 by Kargl and coworkers [24], compounds ML193, ML192 and ML191 by Heynen-Genel et al. [25,26] identified in collaboration with the Molecular Libraries Probe Production Centers Network initiative, and coumarin derivatives by Rempel et al. [27] In addition, some magnolol derivatives have been recently reported to behave as GPR55 antagonist, though retaining activity at additional receptors [28].

The aim of our study was to design and synthesize a series of selective and potent GPR55 agonists which do not interact with various endocannabinoid targets. At first, we utilized the screening results from PubChem bioassay AID 1961 and selected *N*-(4-sulfamoylphenyl)thiourea based structures [CID1792579 (**1**) and CID1252842 (**2**) and CID1011163 (**3**)] as a starting point for ligand development. Consequently, we screened a small set of commercial analogues having similarity with the ligands **1**–**3** for their GPR55 activity by using commercial β-arrestin PathHunter assay. The active compounds were further evaluated by using a recombinant HEK239-GPR55 cell line exhibiting GPR55-mediated effects on calcium signalling [29]. Based on the results, a total of 16 compounds were designed, synthesized and evaluated for their ability to activate the GPR55 receptor. The compounds were not active when tested against various endocannabinoid targets (CB1R, CB2R, FAAH, MGL, ABHD6 and ABHD12), indicating selectivity for the GPR55 receptor.

Overall, we report here the pharmacological evaluation of 27 GPR55 ligands, of which several turned out to be low nanomolar, high potency agonists. Structure–activity relationships (SAR) of the compounds were explored to define important features for receptor activation.

2. Results and discussion

2.1. Search and evaluation of the hit structures

A starting point for the ligand design was found from PubChem bioassay AID 1961 which reports the results of Image-based HTS for selective agonists of GPR55 [20,21]. Two compounds, CID1792579 (**1**) and CID1252842 (**2**) (Fig. 2), were selected among the active compounds based on structural similarity, potency and synthetic feasibility. The assay (AID 1961) also included one inactive compound, CID1011163 (**3**) (Fig. 2), an *N*-unsubstituted sulfonamide analogue of **1** and **2**. All three compounds were first screened by using commercial β-arrestin PathHunter assay and then further

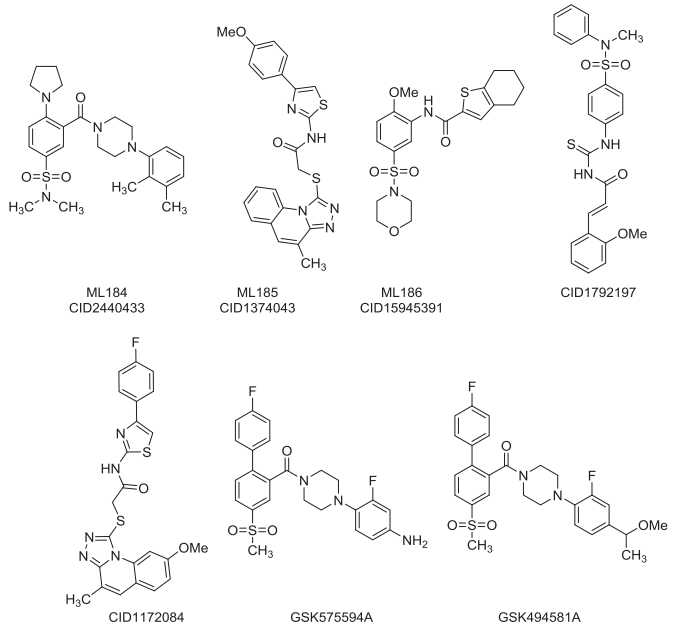

Fig. 1. Some GPR55 agonists mentioned in literature.

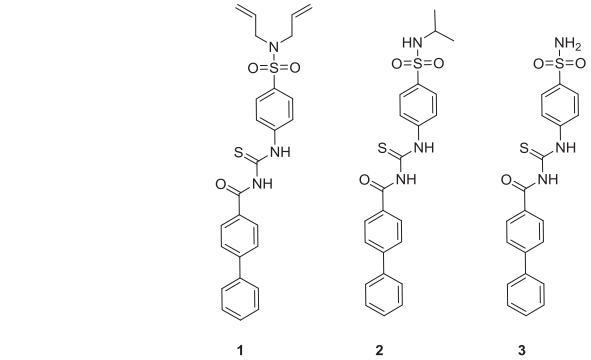

	1 CID1792579	2 CID1252842	3 CID1011163
EC_{50} reported in PubChem AID 1961:	500 nM	500 nM	inactive
PathHunter beta-arrestin screen for GPR55:	119[a] (105, 134)	155[a] (148, 162)	103[a] (83, 122)
Ca^{2+} signaling assay for GPR55, EC_{50}:	11.9 nM[b] (8.4-17.0 nM)	122.3 nM[b] (97.4-153.5 nM)	76.2 nM[b] (40.1-144.8 nM)

Fig. 2. The GPR55 activity data for structures **1**–**3** obtained from PubChem bioassay (AID 1961) [20,21]. (a) GPR55 agonism at 10 μM ligand concentration. Results are reported as a percentage of the luminescence given by the reference compound LPI at 1 μM concentration (mean with range of two experiments performed in duplicate). (b) Measured EC_{50} values for effects on calcium signalling (mean with 95% confidence intervals, derived from concentration-response curves, with each point representing pooled data from 24 individual cells).

evaluated by using a recombinant HEK cell line exhibiting GPR55-mediated effects on calcium signalling (Fig. 2).

To gain more information on the compounds' structural requirements for ligand binding to GPR55, eight close analogues for compounds **1**–**3** were purchased from ChemBridge (**4**–**11**). Compounds **4** and **5** had variations only at the sulfonamide moiety whereas compounds **6**–**11** had variations both at the carboxamide and sulfonamide moieties of the molecules (Table 1). Compounds were tested for their ability to activate GPR55. Various cannabinoid related targets including the CB1 and CB2 receptors, and the enzymes FAAH, MGL, ABHD6, and ABHD12 were also screened at a concentration of 10 μM.

Results for compounds **1**–**3** are shown in Fig. 2 and for compounds **4**–**11** in Table 1. Compound **1** was the most potent analogue with the EC_{50} value of 11.9 nM. Furthermore, the compounds **1**–**5** having variations only at the sulfonamide moiety were active, but replacement of biphenyl moiety with other aryl groups (**6**–**11**) resulted in a marked loss in GPR55 agonist activity. The discrepancies between the results measured in this study and the results reported in PubChem bioassay for compounds **1**–**3**, are likely to reflect different assay conditions. Interestingly, the assumed inactive compound (**3**) according to PubChem seemed to be quite potent (EC_{50} = 76.2 nM) in our assay conditions.

Compounds **3** and **4** were the only compounds in this series to raise selectivity concerns. Namely, compound **3** weakly activated CB1 receptor and inhibited FAAH whereas compound **4** showed only a weak inhibitory effect against FAAH (Supporting information Table S1). Overall, most of the compounds showed some inhibition of ABHD6 and ABHD12 at 10 μM concentration, however, no inhibition was detected at 1 μM concentration. This suggests that the compounds **1**, **2** and **5** are selective agonists of GPR55 over various molecular targets of the endocannabinoid system.

2.2. Design and synthesis of GPR55 agonist analogues

Based on the SAR information obtained from the compounds **1**–**11**, we designed and synthesized series of 16 analogues (**17a-p**, Tables 2 and 3), in which the sulfonamide moiety was varied while the biphenyl carboxamide moiety was kept intact as the biphenyl compounds were the most potent in the screening of commercial compounds (**4**–**11**).

Synthesis of the analogues was based on the methods described in literature [30–35]. Scheme 1 shows the general reaction pathway for the compounds **1** and **17a-p**. At first, primary amines were treated with 4-nitrobenzenesulfonyl chloride (**12a**) or 4-nitrobenzoyl chloride (**12b**) in the presence of pyridine or triethylamine to generate the corresponding (sulfon)amides (**13a-q**). The reduction of nitro group with Sn/HCl gave the corresponding

Table 1
The GPR55 activity data of commercial analogues **4**–**11**.

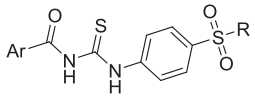

	R	Ar	PathHunter β-arrestin screen for GPR55[a]	Ca^{2+} signalling assay for GPR55[b] EC_{50} (nM)
4	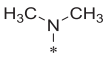	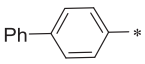	101 (92, 109)	55.7 (36.1–85.8)
5	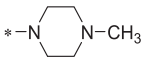	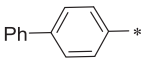	148 (133, 162)	218.0 (128.5–369.9)
6	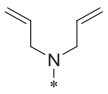	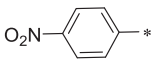	93 (90, 95)	nd
7		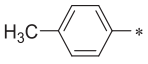	69 (66, 72)	nd
8		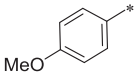	62 (58, 66)	nd
9		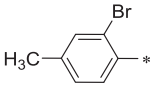	70 (70, 71)	nd
10	NHAc	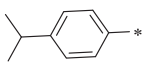	67 (65, 68)	nd
11	NHAc	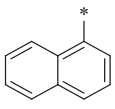	66 (65, 68)	nd

[a] GPR55 agonism at 10 μM ligand concentration. Results are reported as a percentage of the luminescence given by the reference compound LPI at 1 μM concentration (mean with range of two experiments performed in duplicate).

[b] Measured EC_{50} values for effects on calcium signalling (mean with 95% confidence intervals, derived from concentration-response curves, with each point representing pooled data from 24 individual cells).

Table 2
GPR55 agonist analogues with *N*-benzyl group.

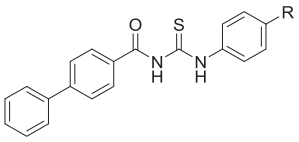

	R	PathHunter β-arrestin screen for GPR55[a]	Ca^{2+} signalling assay for GPR55[b] EC_{50} (nM)
17a	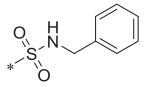	197 (186, 207)	5.6 (2.6–12.9)
17b	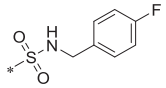	185 (116, 254)	2.0 (1.5–2.8)
17c	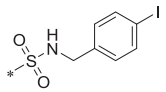	107 (93, 121)	inactive at 10 μM
17d	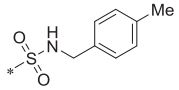	148 (146, 151)	12.4 (8.5–18.1)
17e	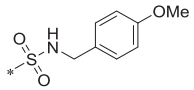	157 (135, 178)	7.7 (4.0–14.8)
17f	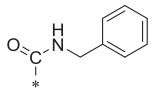	67 (67, 68)	>10 μM

[a,b] as shown in Table 1, nd = not determined.

anilines (**14a-q**). The final products (**1**, **17a-p**) were obtained after the reaction of 4-phenylbenzoyl chloride (**15**) with potassium thiocyanate produced biphenyl-4-carbonyl isothiocyanate (**16**) which was treated with previously synthesized anilines.

2.3. Biological evaluation and SAR of compounds *17a-p*

All compounds **17a-p** were tested for their ability to activate the GPR55 receptor. Commercial β-arrestin PathHunter GPR55 assay was first used to screen the compounds' ability to activate GPR55 at 10 μM concentration, and then all the compounds having an intact biphenyl carboxamide moiety and a promising screening result (>100%) were further evaluated by using a recombinant HEK cell line exhibiting GPR55-mediated effects on calcium signalling. Compounds **17f** and **17k** were also evaluated with the GPR55-HEK cell line as a comparison (screening results 67% and 68%, respectively). The EC_{50} values of *N*-benzyl substituted analogues (**17a-f**) are listed in Table 2, and compounds having other *N*-aryl or *N*-alkyl substitution (**17g-p**) are presented in Table 3. Representative calcium traces and concentration-response curves are shown for the compounds **17d**, **17g**, **17l,** and for the reference compound 1-arachidonoyl-2-hydroxy-*sn*-glycero-3-phosphoinositol (ARA-LPI, EC_{50} = 20.24 nM, 95% CI = 14.66–27.96 nM) in Fig. 3. It's possible to note that the single calcium transient treated with **17d**, **17g** and **17l** does not return to the baseline values because of activation of GPR55 leads to sustained, elevated calcium responses [29]. For the calcium mobilisation assay, where E_{max} values could be determined, all active ligands were full agonists. A general observation was that the most potent GPR55 agonists (**17a-b**, **17e**, **17g** and **17l**) with EC_{50} values below 10 nM are the compounds with *N*-benzyl or *N*-aryl sulfonamide moiety. The unsubstituted *N*-benzyl sulfonamide **17a** was a potent GPR55 agonist (EC_{50} = 5.6 nM) and the potency was increased by a fluorine substituent at the *para* position of the benzyl ring (**17b**, EC_{50} = 2.0 nM). Interestingly, the activity is lost when fluorine is replaced by iodine (**17c**). This may be due to the large atomic size of iodine or different electronic properties as fluorine is a better unconventional hydrogen bond acceptor than iodine. In fact, even a methoxy group in para-position (**17e**, EC_{50} = 7.7 nM) can fit to the binding site and it only slightly decreases the activity compared to **17a** indicating that substituents with hydrogen bond acceptor properties are more tolerable than other groups. The importance of a sulfonamide group was tested by replacing it to an amide group. The change produced an inactive analog **17f**.

N-phenyl (**17g**, EC_{50} = 7.0 nM) and *N*-phenethyl (**17j**, EC_{50} = 39.2 nM) substituents are tolerated almost equally well as *N*-benzyl in **17a** (Table 3). However, the introduction of chlorine (**17h**) or butyl (**17i**) substituents at the para-position of *N*-phenyl group were not favourable for the activity: **17i** was inactive and we were not able to determine EC_{50} value for **17h** even though it gave a promising result in the β-arrestin assay. Furthermore, when we replaced the *N*-phenethyl sulfonamide moiety of **17j** with corresponding amide (**17k**), the activity was lost. The *N*-furanylmethyl substitution in **17l** provide optimal activity (EC_{50} = 2.0 nM), while larger *N*-indolyl ethyl substituent of **17m** was not tolerated. Removal of one allyl from the *N*,*N*-diallyl sulfonamide (**1**), resulted in a slight decrease in GPR55 receptor activity (**17n**, EC_{50} = 19.4 nM). Aliphatic *N*-propyl and *N*-isobutyl substituted compounds **17o** and **17p** produced also fairly potent GPR55 agonists (EC_{50} = 190.3 and 30.9 nM, respectively).

Table 3
GPR55 agonist analogues with other than *N*-benzyl substituent.

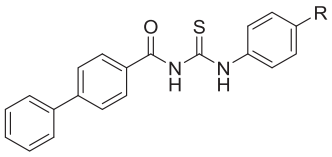

	R	PathHunter β-arrestin screen for GPR55[a]	Ca^{2+} signalling assay for GPR55[b] EC_{50} (nM)
17g	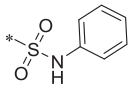	178 (161, 196)	6.2 (3.9–10.0)
17h	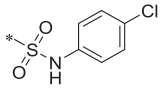	158 (125, 191)	nd*
17i	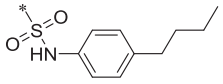	91 (81, 101)	nd
17j	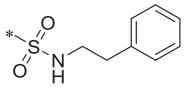	117 (104, 130)	39.2 (23.9–64.4)
17k	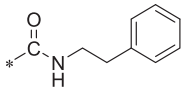	68 (53, 83)	>10 μM
17l	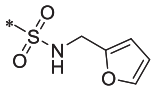	168 (137, 200)	2.0 (1.2–3.3)
17m	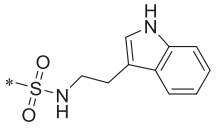	90 (67, 113)	inactive at 10 μM
17n	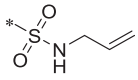	194 (167, 221)	19.4 (13.8–27.4)
17o	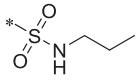	172 (143, 200)	175.7 (117.2–263.4)
17p	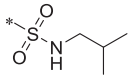	165 (133, 197)	30.9 (22.2–42.9)

[a,b] as shown in Table 1, nd* = not determinable, nd = not determined.

All compounds **17a-p** were inactive when tested against various endocannabinoid related targets (Supporting Information Table S1).

2.4. Molecular modeling

The aim of the modeling conducted in this study was to construct explanatory homology model of GPR55 and to employ the model in molecular docking studies (Fig. 4). Furthermore a comparative molecular field analysis (CoMFA) model was constructed and its main fields were overlaid with model using docking pose of compound **17b** for positioning (see supplementary Fig. S1) [36]. The model of human GPR55 receptor was constructed using homology modeling and the human β_2 adrenergic receptor in an active conformation as a template (sequence identity 24%) as this is the only available GPCR structure in the fully active state. The model has a disulfide bridge between Cys94 in the third transmembrane helix (TMH3) and Cys168 in the second extracellular loop (EC2). This receptor does not have a conserved proline residue in the seventh transmembrane helix (TMH7). Furthermore, the model was utilized in induced-fit docking studies [37]. Kotsikorou et al. reported earlier a homology model of the GPR55 and mapped putative binding site of GPR55 antagonists [26]. In this study, we docked the most potent agonists, such as *N*-benzyl (**17a**), *N*-4-fluorobenzyl (**17b**) and *N*-furanylmethyl (**17l**) analogues in our homology model in order to elucidate the key interactions between the receptor and ligands. Docking suggests that the overall extended shape of the current lipophilic ligand series aligns well between seven transmembrane helixes.

Furthermore, sulfamoyl moiety was found to form hydrogen

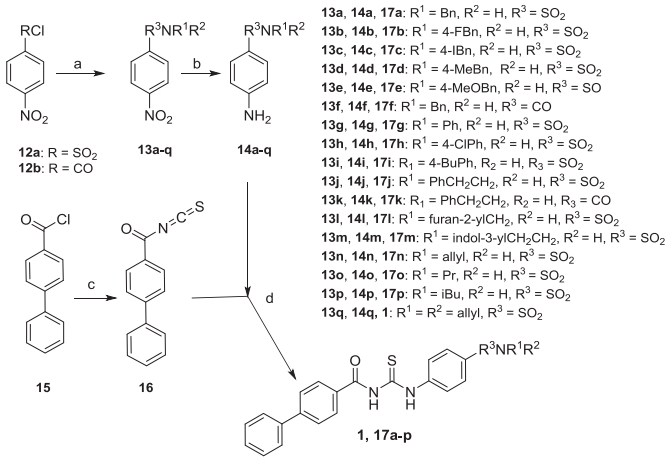

Scheme 1. Synthesis of GPR55 agonist analogues. Reagents and conditions: (a) Amine R_1R_2NH, pyridine, DCM, rt to reflux or amine R_1R_2NH, Et_3N, acetonitrile, reflux; (b) Sn/HCl, EtOH, reflux; (c) KSCN, acetone, reflux; (d) **14a-r**, acetone, reflux.

bond with the polar side chain of N7.43. Placement of positive CoMFA fields confirm that residue N7.43 has an important role for as a hydrogen bond acceptor, as seen in docking results. Placement of the biphenyl moiety between helixes converged well allowing

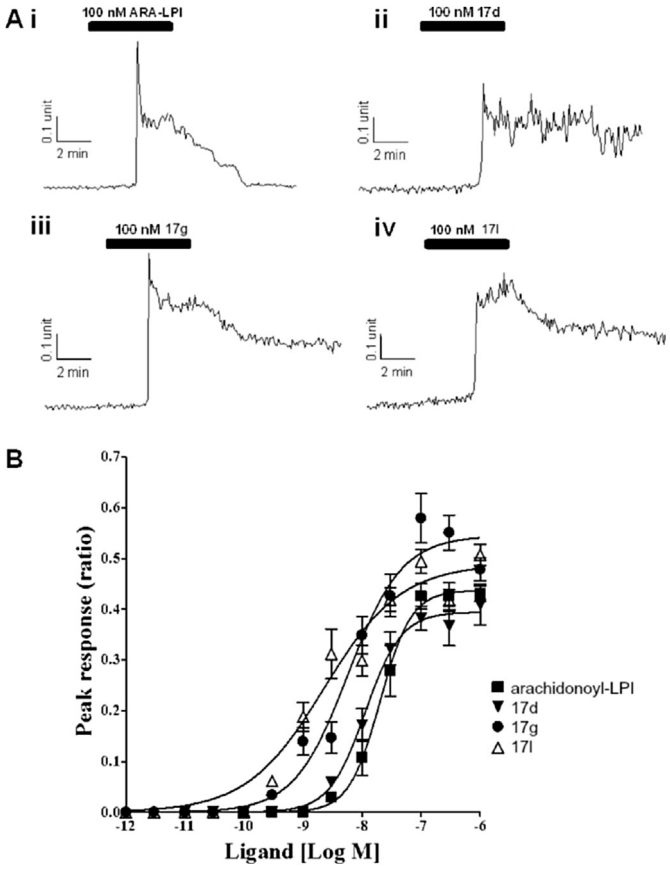

Fig. 3. Calcium transients in hGPR55-HEK293 cells. **Ai**, representative calcium trace from a hGPR55-HEK293 cell challenged with 100 nM ARA-LPI. **Aii**, representative calcium traces of a hGPR55-HEK293 cell treated with a GPR55 agonist with an *N*-benzyl group, 100 nM **17d**. Representative traces of a hGPR55-HEK293 cell challenged with GPR55 agonist analogues with other than *N*-benzyl substituent as follows **Aiii**, 100 nM **17g**; **Aiv**, 100 nM **17l**. **B**, concentration-response curves illustrating the mean peak calcium response data of ARA-LPI (filled squares), **17d** (filled triangles), **17g** (filled circles) and **17l** (open triangles). Data are the mean peak response ± SEM derived from 24 cells, from two independent experiments.

interactions with some phenylalanine F5.47, F6.48, F6.44 and methionine side chains M7.39, M3.36. A favourable steric CoMFA field at the placement of the phenyl linker between sulfamoyl and thiourea moieties suggests that occupying this area is important, which is supported by docking where t-shaped π-interaction with tyrosine Y3.32 is constantly found. Interestingly, the benzyl (**17a**) and the p-fluoro benzyl (**17b**) derivatives are docked well between TMH2 and TMH3, whereas the p-iodobenzyl substituted compound **17c** has adopted a different orientation at the direction of TMH4 and extracellular loop (EC2) (Fig. 4). This is most probably caused by much larger van der Waals radius of iodine, and this assumption is supported by overlap of iodine with sterically disallowed region in our CoMFA model. When bulky n-butylbenzyl-substituted compound **17i** was docked between TMH2 and TMH3, it induced additional steric strain when compared to **17b**. Comparison of the compounds **17a** and **17f** gives a clue about the structural basis for the replacement of sulfonamide linkage with amide. According to dockings sulfonamide group is typically able to accept two hydrogen bonds from opposite sides of binding site and its NH group is also able to act as a donor in some cases. As a comparison, compound **17f** was seen to act only as a single hydrogen bond accepting group, with one of the residues Q2.65, Q7.36 or E3.2. Secondly, only Z-conformations were found for amide bond which oriented *N*-benzyl substituent towards TMH4 and extracellular loop EC2 similarly to the inactive compound **17c**. As a consequence, bulky groups at the para position of *N*-phenyl ring seem to be sterically unfavourable and specific hydrogen bonding properties of the sulfonamide group seem to be the key to initiate signalling pathways.

3. Conclusions

In summary, we generated analogues of the hit compounds **1**–**3**, studied their structure–activity relationships, and created a series of highly potent GPR55 agonists. The most potent agonists among the series were **17a-b**, **17e**, **17g** and **17l** with EC_{50} values below 10 nM.

The hit compounds **1**–**3** were further modified by varying the sulfonamide moiety and keeping the biphenyl carboxamide moiety intact. Overall, the *N*-aryl substituted sulfonamides proved to be the most potent compounds. In addition, the *N*-alkyl substitution was well tolerated as illustrated by the compounds **2**–**4**, **17o** and **17p**. However, compounds **3** and **4** having small aliphatic sulfonamide moieties were weakly interacting with other endocannabinoid targets. Compound **3** weakly activated CB1 receptor and inhibited FAAH, whereas compound **4** just weakly inhibited FAAH. All designed analogues **17a-p** were selective for GPR55 over the other tested targets.

According to homology modeling and docking studies, the active compounds resulted a good convergence of docking poses in between TMH-helixes. Polar parts of the ligands are able to form hydrogen bond contacts with important residues. In addition, both docking and CoMFA studies suggest that increased in size of the halogen substituent at the para position of the sulfamoylphenyl moiety seem to cause the activity cliff.

The GPR55 activity of the ligands was evaluated using a β-arrestin screen at a fixed concentration (10 μM) or changes in intracellular calcium levels to generate concentration-response data. The latter responses are predominantly mediated by the $G\alpha_{12/13}$ pathway.[29] The results generated using these two approaches were generally in good agreement, however modest differences were observed, for example with **1** (119%, EC_{50} = 11.9 nM) and **3** (103%, EC_{50} = 76.2 nM) with some which may indicate agonist biased signalling favouring either $G\alpha_{12/13}$ or β-arrestin outputs.

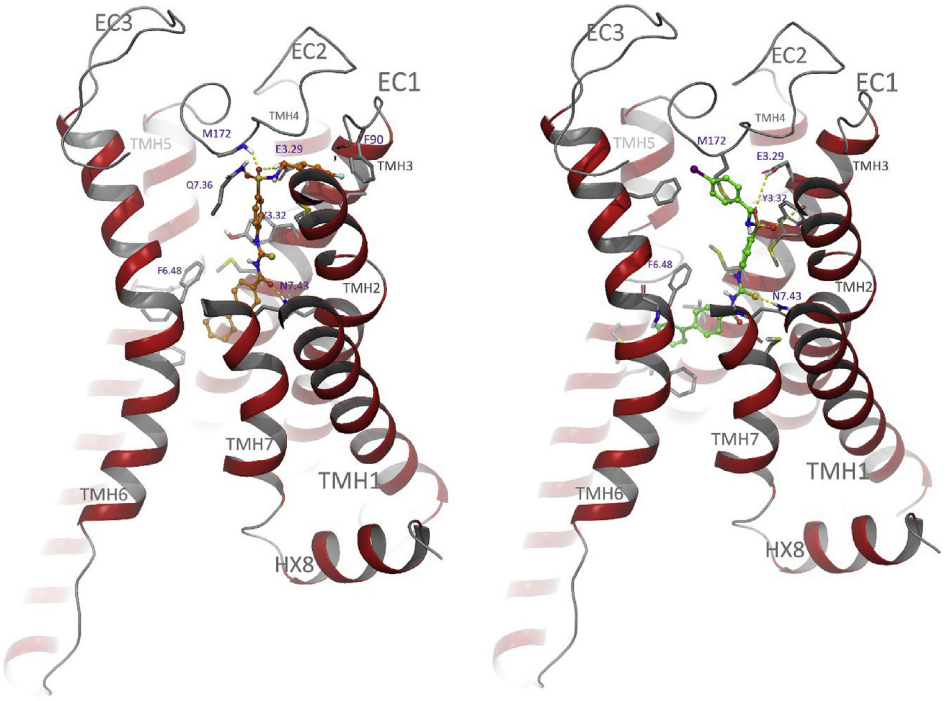

Fig. 4. The most favourable induced fit docking poses of compounds **17b** (left panel, orange carbons) and **17c** (right panel, green carbons) to homology model of active GPR55 showing that in docking compounds orientate similarly between helixes but the N-benzyl substituent is sensitive for the size of the substituent in para position. Key interacting residues are depicted. The upper parts of the TMH7 and TMH1 have been omitted for clarity. (For interpretation of the references to colour in this figure legend, the reader is referred to the web version of this article.)

4. Experimental section

4.1. Commercial compounds

Compounds **2**–**11** were purchased from ChemBridge Corporation (CA, USA) and they were mainly used to verify the results of the hit structures found from PubChem bioassay and to get more information for the basis of ligand design. The purity of these compounds was ≥90% according to the manufacturer and no further analyses were made.

4.2. Novelty of the structures

We examined which compounds are either new or known using SciFinder. Compounds **2**–**11** are known and were purchased from ChemBridge. Synthesized compounds **17b-f**, **17h-i**, **17k**, **17m**, **17p** are new compounds. Synthesized compounds **17a** (CAS 817635-73-7), **17j** (CAS 651297-79-9), **17l** (CAS 925198-41-0), **17n** (CAS 819817-62-4) and **17o** (CAS 875010-19-8) are known commercial compounds, but they do not appear in the literature. Synthesized compounds **17g** (CAS 651297-31-3) and **1** (CAS 791795-02-3) are known commercial compounds that appear in the patents (WO 2011022393 and US 20090163545, respectively) but no synthesis procedures or characterizations are described.

4.3. Comparative modeling of GPR55

The sequence of human GPR55 receptor was obtained from UniProt database (Q9Y2T6) and used to align with the available templates with MOE Molecular Environment [38] using GPCR module. Molecular alignment was corrected manually to satisfy conserved residues in the transmembrane helices. Human β2 adrenergic receptor in an active conformation (in complex with Gs protein), PDB ID: 3SN6 [39] was used as a template as this template is characterized by the highest sequence identity to the target among active state crystal structures, and it is recognized to be in fully active state in contrast to the adenosine receptor templates. Homology modeling with Modeller v. 9.10 [40] was used to construct a populations of 200 models. Subsequent MD-slow refinement of short loops with Modeller was applied. The best models were selected on the basis of the lowest values of Modeller objective function as well as the discrete optimized protein energy (DOPE) option in Modeller (a pseudo-energy term based on a distance-dependent statistical potential) [41]. The quality of the final model was assessed with Annolea [42], Verify3D [43] and ProCheck [44]. Pymol v.1.5.0.3 [45] and SPDBV v. 4.10 [46] were used for visualization of results.

4.4. Molecular docking

Molecular docking studies were performed using Schrödinger Maestro software package [47]. Structures of small molecules were prepared using the LigPrep module. The structure of biomolecule was pre-processed using the protein preparation wizard in order to optimize the hydrogen bonding network [48]. Molecular docking studies were done using Induced Fit docking protocol where the grid box was centred using proposed active site residues [37]. Prime module was used to alter side chain conformations between TMH-helixes to be more suitable for initial docking. Initial docking poses were generated using Glide after which residues close to the ligand pose (5 Å) were further refined using Prime. Re-docking was performed using SP settings of Glide.

4.5. CoMFA

The structural features of a series of GPR55 binding compounds

(n = 28 of which 26 was used in the final model) were correlated with experimentally determined GPR55 effective concentration (EC_{50}) using CoMFA approach [49]. Prior to CoMFA calculations compounds were superimposed based on the docking poses of most active compounds with the assistance of Schrödinger Maestro flexible ligand alignment functionality and manual adjustments when needed. ESP-charges of ligands were calculated using Jaguar software [37] using single point DFT calculations (B3LYP) with MSV basis set in order to achieve better description of electrostatics. Alignment and the charge definitions were followed by generating electrostatic and steric interaction fields for the using Coulomb and Lennard-Jones potentials. The compounds were positioned in a regular three-dimensional cubic grid with 2 Å spacing. The interaction energies between the compound and probe atoms were calculated in each grid point. Finally, the relationships of the intermolecular interaction fields with biological activity (nanomolar log-EC_{50} concentration) were analyzed by multivariate statistical technique, PLS. For more details see the supplementary Fig. S2.

4.6. General synthetic procedures

Commercially available chemicals were used without further purification. Solvents were dried on sieves (3 Å or 4 Å) before use. Reactions were monitored by thin layer chromatography (TLC) which was performed on Merck silica gel F254 precoated aluminium sheets. $CHCl_3$/MeOH (95:5) was used as an eluent and spots were detected by UV light and ninhydrin. Intermediates and products could be purified by column chromatography using Merck Silica Gel 60 (63–200 μm), recrystallization and/or washing with hexane. Elution of column chromatography was performed using $CHCl_3$ (or DCM) or $CHCl_3$/MeOH (or DCM/MeOH) with an increasing gradient of MeOH. Recrystallization was done from DCM/hexane, EA/hexane or DCM/acetone/hexane. Yields were not optimized.

NMR spectra were recorded on a Bruker Avance instrument (500.1 MHz for ^{1}H, 125.8 MHz for ^{13}C). Chemical shifts are reported in δ (ppm) values with tetramethylsilane or the solvent resonance as an internal standard. Coupling constants J are given in Hz. Multiplicities are described as s (singlet), d (doublet), t (triplet), q (quartet), h (heptet), sxt (sextet), tt (triplet of triplets), dq (doublet of quartets), dt (doublet of triplets), ddd (doublet of doublet of doublets), ddt (doublet of doublet of triplets), m (multiplet), br (broad peak). ESI mass spectra were performed on Finnigan MAT LCQ quadrupole ion trap mass spectrometer. Elemental analyses were carried out using a ThermoQuest CE Instruments EA 1110 CHNS–O elemental analyzer. The purity (≥95%) of compounds **1**, **17a**, **17l** and **17p** were determined also by using Agilent 1100 series HPLC with DAD detector (254 nm). Column: Zorbax Eclipse XBD-C18, 4.6 × 50 mm, 1.8 μm, Agilent Technologies. Eluent: ACN/acetate buffer pH 5 (60:40), MeOH/acetate buffer pH 5 (60:40) or ACN/water (60:40).

Synthesis procedures of all compounds are based on methods reported in literature [30–35]. The final products were obtained after three steps, and most of the reactions follow general procedures A (step 1), B (step 2) and C (step 3) described below.

4.6.1. General procedure A (step 1)

4-Nitrobenzenesulfonyl chloride (**12a**, 1.8 mmol, 1 eq) or 4-nitrobenzoyl chloride (**12b**, 1.8 mmol, 1 eq) in dry DCM (25 mL) was added to a mixture of an appropriate amine (1.1–1.6 eq) and pyridine (1–1.6 eq) in dry DCM (25 mL). The reaction mixture was stirred at a sufficient temperature (rt to refluxing). When TLC indicated the disappearance of the starting material, the mixture was washed with 1 M HCl and the organic phase was dried with Na_2SO_4. The solvent was finally evaporated and the product was purified with column chromatography if needed.

4.6.2. General procedure B (step 2)

Concentrated HCl (10–15 ml) was added slowly to a mixture of 4-nitrobenzenesulfonamide or 4-nitrobenzamide analog (**13a-q**, 1.4 mmol, 1 eq) and Sn granules (2–2.5 eq) in ethanol (10 mL). The reaction mixture was refluxed for 3.5–6 h. When the TLC plate showed that there is no more starting material left, the reaction mixture was cooled down to rt. NaOH (30% or 5 M, aq) was added to the mixture until it became basic. The mixture was extracted with EA or DCM and the organic layer was dried with Na_2SO_4. The solvent was evaporated. The product was purified with column chromatography when required.

4.6.3. General procedure C (step 3)

4-Phenylbenzoyl chloride (**15**, 1.2 mmol, 1–1.2 eq) in acetone (10 mL) was added slowly to a mixture of potassium thiocyanate (1–1.2 eq) in acetone (10 mL). The reaction mixture was refluxed 1.5–3 h and the reaction was monitored by TLC. The reaction mixture was cooled down to rt and an appropriate benzenesulfonamide or benzamide analog (**14a-q**, 1 eq) in acetone (10 mL) was slowly added. The reaction mixture was refluxed for 2–4 h or overnight. When starting material was disappeared (detected by TLC plate), the mixture was poured on ice cold water which pH was adjusted to 5 with HCl. If the product crystallized, it was filtered and washed with small amount of cold water. Otherwise the mixture was extracted with EA. The product was purified by column chromatography, recrystallization or washing with hexane.

4.6.4. Compounds ***13a-q***, ***14a-q***, ***1*** and ***17a-p***

*4.6.4.1. N-Benzyl-4-nitrobenzenesulfonamide (**13a**).* From 4-nitrobenzenesulfonyl chloride (**12a**, 1.0 g, 4.5 mmol), benzylamine (0.55 ml, 5.0 mmol) and pyridine (0.40 ml, 5.0 mmol) with general procedure A. Refluxed for 1 h and stirred overnight at rt. Light yellow solid (0.71 g, 54%). ^{1}H NMR (DMSO-d_6): δ 4.07 (2H, d, J = 6.1 Hz), 7.19–7.28 (5H, m), 8.00 (2H, d, J = 8.8 Hz), 8.36 (2H, d, J = 8.8 Hz), 8.54 (1H, t, J = 6.1 Hz).

*4.6.4.2. N-(4-Fluorobenzyl)-4-nitrobenzenesulfonamide (**13b**).* From **12a** (0.50 g, 2.3 mmol), 4-fluorobenzylamine (0.31 ml, 2.7 mmol) and pyridine (0.22 ml, 2.7 mmol) with general procedure A. Refluxed overnight. Light yellow solid (0.44 g, 63%). ^{1}H NMR (DMSO-d_6): δ 4.06 (2H, s), 7.08 (2H, t, J = 8.9 Hz), 7.24 (2H, dd, J = 8.9, 5.5 Hz), 8.00 (2H, d, J = 9.0 Hz), 8.36 (2H, d, J = 9.0 Hz), 8.56 (1H, s).

*4.6.4.3. N-(4-Iodobenzyl)-4-nitrobenzenesulfonamide (**13c**).* From **12a** (0.25 g, 1.1 mmol), 4-iodobenzylamine hydrochloride (0.30 g, 1.1 mmol), triethylamine (0.16 ml, 1.1 mmol) and pyridine (0.23 ml, 2.8 mmol) with general procedure A. Refluxed overnight. White solid (0.35 g, 74%). ^{1}H NMR (DMSO-d_6): δ 4.03 (2H, s), 7.01 (2H, d, J = 8.3 Hz), 7.60 (2H, d, J = 8.3 Hz), 7.97 (2H, d, J = 8.9 Hz), 8.35 (2H, d, J = 8.9 Hz), 8.58 (1H, s).

*4.6.4.4. N-(4-Methylbenzyl)-4-nitrobenzenesulfonamide (**13d**).* From **12a** (0.50 g, 2.3 mmol), 4-methylbenzylamine (0.35 ml, 2.7 mmol) and pyridine (0.22 ml, 2.7 mmol) with general procedure A. Refluxed for 6 h. Light yellow solid (0.44 g, 64%). ^{1}H NMR (DMSO-d_6): δ 2.23 (3H, s), 4.01 (2H, s), 7.06 (4H, m), 7.98 (2H, d, J = 8.8 Hz), 8.35 (2H, d, J = 8.8 Hz), 8.50 (1H, s).

*4.6.4.5. N-(4-methoxybenzyl)-4-nitrobenzenesulfonamide (**13e**).* From **12a** (0.40 g, 1.8 mmol), 4-methoxybenzylamine (0.26 ml, 2.0 mmol) and pyridine (0.16 ml, 2.0 mmol) with general procedure A. Refluxed overnight. Yellow solid (0.37 g, 64%). ^{1}H NMR (DMSO-

d_6): δ 3.69 (3H, s), 3.99 (2H, d, J = 6.1 Hz), 6.79 (2H, d, J = 8.5 Hz), 7.10 (2H, d, J = 8.5 Hz), 7.97 (2H, d, J = 8.8 Hz), 8.34 (2H, d, J = 8.8 Hz), 8.45 (1H, t, J = 6.1 Hz).

*4.6.4.6. N-Benzyl-4-nitrobenzamide (**13f**).* Benzylamine (0.41 ml, 3.8 mmol) was dissolved in DCM (25 mL), cooled to 0 °C and *N*-methylmorpholine (0.90 ml, 8.2 mmol) was added. 4-Nitrobenzoyl chloride (**12b**) in DCM (25 mL) was added slowly to the solution. The mixture was stirred overnight at rt and washed with 2 M HCl (x3), sat. $NaHCO_3$ (x1) and brine (x1). The organic layer was dried with Na_2SO_4 and the solvent was evaporated. White solid (0.89 g, 92%). ^{1}H NMR (DMSO-d_6): δ 4.51 (1H, d, J = 5.9 Hz), 7.26 (1H, m), 7.34 (4H, d, J = 4.4 Hz), 8.12 (2H, d, J = 8.8 Hz), 8.33 (2H, d, J = 8.8 Hz), 9.37 (1H, t, J = 5.8 Hz).

*4.6.4.7. 4-Nitro-N-phenylbenzenesulfonamide (**13g**).* From **12a** (1.07 g, 4.8 mmol), aniline (0.47 ml, 5.1 mmol) and pyridine (0.40 ml, 4.9 mmol) with general procedure A. Refluxed for 4.5 h. Reddish solid (1.31 g, 98%). ^{1}H NMR (DMSO-d_6): δ 7.10 (3H, m), 7.25 (2H, m), 7.99 (2H, d, J = 8.9 Hz), 8.37 (2H, d, J = 8.9 Hz), 10.58 (1H, s).

*4.6.4.8. N-(4-Chlorophenyl)-4-nitrobenzenesulfonamide (**13h**).* From **12a** (1.0 g, 4.5 mmol), 4-chloroaniline (0.69 g, 5.4 mmol) and pyridine (0.44 ml, 5.4 mmol) with general procedure A. Stirred at rt for overnight. Red solid (1.46 g, 100%). ^{1}H NMR (DMSO-d_6): δ 7.11 (2H, d, J = 8.8 Hz), 7.33 (2H, d, J = 8.8 Hz), 7.98 (2H, d, J = 8.8 Hz), 8.38 (2H, d, J = 8.8 Hz), 10.75 (1H, s).

*4.6.4.9. N-(4-butylphenyl)-4-nitrobenzenesulfonamide (**13i**).* From **12a** (1.0 g, 4.5 mmol), 4-butylaniline (0.86 ml, 5.4 mmol) and pyridine (0.44 ml, 5.4 mmol) with general procedure A. Stirred at rt for overnight. Red solid (1.51 g, 100%). ^{1}H NMR ($CDCl_3$): δ 0.90 (3H, t, J = 7.3 Hz), 1.31 (2H, m), 1.54 (2H, m), 2.55 (2H, t, J = 7.7 Hz), 6.80 (1H, s), 6.97 (2H, d, J = 8.3 Hz), 7.07 (2H, d, J = 8.3 Hz), 7.91 (2H, d, J = 8.9 Hz), 8.27 (2H, d, J = 8.9 Hz).

*4.6.4.10. 4-Nitro-N-phenethylbenzenesulfonamide (**13j**).* From **12a** (0.50 g, 2.3 mmol), phenethylamine (0.28 ml, 2.3 mmol) and pyridine (0.19 ml, 2.3 mmol) with general procedure A. Refluxed for 4 h. Light yellow solid (0.37 g, 54%). ^{1}H NMR (DMSO-d_6): δ 2.69 (2H, t, J = 7.4 Hz), 3.04 (2H, m), 7.15–7.20 (3H, m), 7.25 (2H, m), 8.00 (2H, d, J = 8.8 Hz), 8.12 (1H, t, J = 5.5 Hz, 8.38 (2H, d, J = 8.8 Hz).

*4.6.4.11. 4-Nitro-N-phenethylbenzamide (**13k**).* Prepared as the compound **13f** from phenethylamine (0.41 ml, 3.2 mmol), N-methylmorpholine (0.36 ml, 3.2 mmol) and **12b**. Light yellow solid (0.63 g, 87%). ^{1}H NMR (DMSO-d_6): δ 2.87 (2H, t, J = 7.4 Hz), 3.52 (2H, dt, J = 7.4, 5.6 Hz), 7.18–7.33 (5H, m), 8.04 (2H, d, J = 8.9 Hz), 8.31 (2H, d, J = 8.9 Hz), 8.90 (1H, t, J = 5.5 Hz).

*4.6.4.12. N-(Furan-2-ylmethyl)-4-nitrobenzenesulfonamide (**13l**).* From **12a** (0.50 g, 2.3 mmol), furfurylamine (0.28 ml, 3.2 mmol) and pyridine (0.22 ml, 2.7 mmol) with general procedure A. Refluxed for 6 h. Light yellow solid (0.46 g, 72%). ^{1}H NMR (DMSO-d_6): δ 4.11 (2H, d, J = 5.9 Hz), 6.16 (1H, dd, J = 3.2, 0.8 Hz), 6.25 (1H, dd, J = 3.2, 1.9 Hz), 7.42 (1H, dd, J = 1.9, 0.9 Hz), 7.97 (2H, d, J = 9.0 Hz), 8.35 (2H, d, J = 9.0 Hz), 8.59 (1H, t, J = 5.9 Hz).

*4.6.4.13. N-(2-(1H-Indol-3-yl)ethyl)-4-nitrobenzenesulfonamide (**13m**).* From **12a** (0.50 g, 2.3 mmol), tryptamine (0.43 g, 2.7 mmol) and pyridine (0.22 ml, 2.7 mmol) with general procedure A. Refluxed for 5 h. Orange solid (0.45 g, 58%). ^{1}H NMR (DMSO-d_6): δ 2.80 (2H, t, J = 7.3 Hz), 3.12 (2H, br s), 6.93 (1H, t, J = 7.5 Hz), 7.01 (1H, t, J = 7.5 Hz), 7.09 (1H, d, J = 2.0 Hz), 7.25 (2H, d, J = 8.0 Hz), 7.36 (2H, d, J = 7.8 Hz), 7.91 (2H, d, J = 8.7 Hz), 8.10 (1H, s), 8.26 (2H, d, J = 8.7 Hz), 10.77 (1H, s).

*4.6.4.14. N-Allyl-4-nitrobenzenesulfonamide (**13n**).* From **12a** (0.40 g, 1.8 mmol), allylamine (0.15 ml, 2.0 mmol) and pyridine (0.16 ml, 2.0 mmol) with general procedure A. Refluxed overnight. Light orange solid (0.29 g, 66%). ^{1}H NMR (DMSO-d_6): δ 3.50 (2H, s), 5.03 (1H, dq, J = 10.3, 1.5 Hz), 5.14 (1H, dq, J = 17.1, 1.7 Hz), 5.66 (1H, ddt, J = 17.1, 10.3, 5.3 Hz), 8.05 (2H, d, J = 9.1 Hz), 8.20 (1H, s), 8.42 (2H, d, J = 9.1 Hz).

*4.6.4.15. 4-Nitro-N-propylbenzenesulfonamide (**13o**).* From **12a** (1.01 g, 4.6 mmol), n-propylamine (0.60 ml, 7.3 mmol) and pyridine (0.60 ml, 7.5 mmol) with general procedure A. Stirred at rt for overnight. Yellow solid (1.07 g, 96%) and it was used without further purification. ^{1}H NMR ($CDCl_3$): δ 0.89 (3H, t, J = 7.4 Hz), 1.52 (2H, m), 3.00 (2H, m), 4.78 (1H, t, J = 5.5 Hz), 8.07 (2H, d, J = 8.8 Hz), 8.37 (2H, d, J = 8.8 Hz).

*4.6.4.16. N-isobutyl-4-nitrobenzenesulfonamide (**13p**).* From **12a** (1.0 g, 4.5 mmol), isobutylamine (0.54 ml, 5.4 mmol) and pyridine (0.44 ml, 5.4 mmol) with general procedure A. Stirred at rt for overnight. Light yellow solid (0.75 g, 64%). ^{1}H NMR (DMSO-d_6): δ 0.81 (6H, d, J = 6.7 Hz), 1.63 (1H, m), 2.61 (2H, t, J = 6.4 Hz), 7.97 (1H, t, J = 6.0 Hz), 8.04 (2H, d, J = 8.9 Hz), 8.41 (2H, d, J = 8.9 Hz).

*4.6.4.17. N,N-diallyl-4-nitrobenzenesulfonamide (**13q**).* **12a** (1.0 g, 4.5 mmol) in acetonitrile was added to a mixture of diallylamine (0.67 ml, 5.4 mmol) and triethylamine (0.63 ml, 4.5 mmol) in acetonitrile. The mixture was refluxed for 6 h. The solvent was evaporated and the residue was dissolved in $CHCl_3$ and the solution was washed with 1 M HCl and water. The organic layer was dried with Na_2SO_4 and the solvent was finally evaporated. Yellow solid (1.46 g, 86%). ^{1}H NMR ($CDCl_3$): δ 3.88 (4H, d, J = 6.2 Hz), 5.17 (2H, dq, J = 10.2, 1.1 Hz), 5.19 (2H, dq, J = 16.9, 1.4 Hz), 5.58 (2H, ddt, J = 16.9, 10.2, 6.3 Hz), 8.01 (2H, d, J = 9.1 Hz), 8.36 (2H, d, J = 9.1 Hz).

*4.6.4.18. 4-Amino-N-benzylbenzenesulfonamide (**14a**).* From **13a** (0.71 g, 2.4 mmol) with general procedure B. Yellow solid (0.40 g, 63%) that was used without further purification. ^{1}H NMR (DMSO-d_6): δ 3.87 (2H, d, J = 5.7 Hz), 5.91 (2H, s), 6.61 (2H, d, J = 8.7 Hz), 7.20–7.31 (5H, m), 7.44 (2H, d, J = 8.7 Hz), 7.61 (1H, t, J = 5.8 Hz).

*4.6.4.19. 4-Amino-N-(4-fluorobenzyl)benzenesulfonamide (**14b**).* From **13b** (0.44 g, 1.4 mmol) with general procedure B. Light yellow solid (0.35 g, 88%) that was used without further purification. ^{1}H NMR (DMSO-d_6): δ 3.86 (2H, s), 5.92 (2H, s), 6.60 (2H, d, J = 8.7 Hz), 7.10 (2H, t, J = 8.8 Hz), 7.27 (2H, dd, J = 8.8, 5.7 Hz), 7.42 (2H, d, J = 8.7 Hz), 7.67 (1H, br s).

*4.6.4.20. 4-Amino-N-(4-iodobenzyl)benzenesulfonamide (**14c**).* From **13c** (0.35 g, 0.84 mmol) with general procedure B. White solid (0.29 g, 89%) that was used without further purification. ^{1}H NMR (DMSO-d_6): δ 3.82 (2H, s), 5.92 (2H, s), 6.60 (2H, d, J = 8.7 Hz), 7.06 (2H, d, J = 8.3 Hz), 7.42 (2H, d, J = 8.7 Hz), 7.64 (2H, d, J = 8.3 Hz).

*4.6.4.21. 4-Amino-N-(4-methylbenzyl)benzenesulfonamide (**14d**).* From **13d** (0.44 g, 1.4 mmol) with general procedure B. Light yellow solid (0.67 g, 100%).^{1}H NMR (DMSO-d_6): δ 2.26 (3H, s), 3.82 (2H, s), 5.91 (2H, s), 6.64 (2H, d, J = 8.4 Hz), 7.11 (4H, br m), 7.45 (2H, d, J = 8.4 Hz), 7.61 (1H, br s).

*4.6.4.22. 4-Amino-N-(4-methoxybenzyl)benzenesulfonamide (**14e**).* From **13e** (0.37 g, 1.1 mmol) with general procedure B. Brown solid (0.22 g, 66%). ^{1}H NMR (DMSO-d_6): δ 3.72 (3H, s), 3.79 (2H, d, J = 6.3 Hz), 5.90 (2H, s), 6.60 (2H, d, J = 8.4 Hz), 6.84 (2H, d,

J = 8.3 Hz), 7.14 (2H, d, J = 8.3 Hz), 7.43 (2H, d, J = 8.4 Hz), 7.51 (1H, t, J = 6.2 Hz).

*4.6.4.23. 4-Amino-N-benzylbenzamide (**14f**).* From **13f** (0.89 g, 3.5 mmol) with general procedure B. Light yellow solid (0.67 g, 85%). ^{1}H NMR (DMSO-d_6): δ 4.42 (2H, d, J = 6.0 Hz), 5.60 (2H, s), 6.54 (2H, d, J = 8.6 Hz), 7.21 (1H, m), 7.29 (4H, m), 7.61 (2H, d, J = 8.6 Hz), 8.54 (1H, t, J = 5.9 Hz).

*4.6.4.24. 4-Amino-N-phenylbenzenesulfonamide (**14g**).* From **13g** (1.17 g, 4.2 mmol) with general procedure B. Solid (1.03 g, 99%) that was used without further purification. ^{1}H NMR (DMSO-d_6): δ 5.85 (2H, s), 6.50 (2H, d, J = 8.7 Hz), 6.88 (1H, t, J = 7.4 Hz), 7.01 (2H, d, J = 7.6 Hz), 7.14 (2H, m), 7.37 (2H, d, J = 8.7 Hz).

*4.6.4.25. 4-Amino-N-(4-chlorophenyl)benzenesulfonamide (**14h**).* From **13h** (1.41 g, 4.5 mmol) with general procedure B. White solid (1.25 g, 98%) that was used without further purification. ^{1}H NMR (DMSO-d_6): δ 5.99 (2H, s), 6.53 (2H, d, J = 8.6 Hz), 7.06 (2H, d, J = 8.8 Hz), 7.26 (2H, d, J = 8.8 Hz), 7.37 (2H, d, J = 8.6 Hz), 10.0 (1H, s).

*4.6.4.26. 4-Amino-N-(4-butylphenyl)benzenesulfonamide (**14i**).* From **13i** (1.51 g, 4.5 mmol) with general procedure B. Light yellow solid (1.50 g, 100%) that was used without further purification. ^{1}H NMR (DMSO-d_6): δ 0.85 (3H, t, J = 7.3 Hz), 1.24 (2H, m), 1.45 (2H, m), 2.43 (2H, t, J = 7.6 Hz), 5.89 (2H, s), 6.50 (2H, d, J = 8.5 Hz), 6.90–7.10 (4H, m), 7.34 (2H, d, J = 8.5 Hz).

*4.6.4.27. 4-Amino-N-phenethylbenzenesulfonamide (**14j**).* From **13j** (0.37 g, 1.2 mmol) with general procedure B. Yellow solid (0.39 g, 100%) that was used without further purification. ^{1}H NMR (DMSO-d_6): δ 2.64 (2H, t, J = 7.7 Hz), 2.85 (2H, dt, J = 7.7, 5.8 Hz), 5.92 (2H, s), 6.60 (2H, d, J = 8.6 Hz), 7.12 (2H, d, J = 8.2 Hz), 7.20 (1H, t, J = 6.3 Hz), 7.26 (2H, t, J = 7.6 Hz), 7.40 (2H, d, J = 8.6 Hz).

*4.6.4.28. 4-Amino-N-phenethylbenzamide (**14k**).* From **13k** (0.63 g, 2.3 mmol) with general procedure B. Yellow solid (0.54 g, 97%) that was used without further purification. ^{1}H NMR (DMSO-d_6): δ 2.79 (2H, t, J = 7.5 Hz), 3.41 (2H, dt, J = 7.5, 5.7 Hz), 5.74 (2H, s), 6.51 (2H, d, J = 8.7 Hz), 7.15–7.31 (5H, m), 7.53 (2H, d, J = 8.7 Hz), 8.83 (1H, t, J = 5.6 Hz).

*4.6.4.29. 4-Amino-N-(furan-2-ylmethyl)benzenesulfonamide (**14l**).* From **13l** (0.46 g, 1.6 mmol) with general procedure B. Yellow solid (0.69 g, 100%). ^{1}H NMR (DMSO-d_6): δ 3.87 (2H, s), 5.94 (2H, s), 6.17 (1H, dq, J = 3.3, 0.8 Hz), 6.34 (1H, dd, J = 3.0, 1.8 Hz), 6.57–6.60 (1H, m), 6.61 (2H, d, J = 8.7 Hz), 7.42 (2H, d, J = 8.7 Hz), 7.52 (1H, dd, J = 1.8, 0.8 Hz), 7.65 (1H, br s).

*4.6.4.30. N-(2-(1H-Indol-3-yl)ethyl)-4-aminobenzenesulfonamide (**14m**).* From **13m** (0.45 g, 1.3 mmol) with general procedure B. Light orange solid (0.43 g, 100%). ^{1}H NMR (DMSO-d_6): δ 2.75 (2H, m), 2.91 (2H, m), 5.90 (2H, s), 6.60 (2H, d, J = 8.7 Hz), 6.96 (1H, t, J = 7.8 Hz), 7.04 (1H, t, J = 7.8 Hz), 7.10 (1H, d, J = 2.2 Hz), 7.23 (1H, t, J = 6.1 Hz), 7.31 (1H, d, J = 8.1 Hz), 7.37 (1H, d, J = 7.6 Hz), 7.43 (2H, d, J = 8.7 Hz), 10.80 (1H, s).

*4.6.4.31. N-Allyl-4-aminobenzenesulfonamide (**14n**).* From **13n** (0.29 g, 1.2 mmol) with general procedure B. Light orange solid (0.30 g, 100%) that was used without further purification. ^{1}H NMR (DMSO-d_6): δ 3.31 (2H, br s), 5.01 (1H, dq, J = 10.2, 1.6 Hz), 5.12 (1H, dq, J = 17.2, 1.7 Hz), 5.66 (1H, ddt, J = 17.2, 10.3, 5.6 Hz), 5.91 (2H, s), 6.60 (2H, d, J = 8.6 Hz), 7.27 (1H, s), 7.40 (2H, d, J = 8.6 Hz).

*4.6.4.32. 4-Amino-N-propylbenzenesulfonamide (**14o**).* From **13o** (0.75 g, 3.1 mmol) with general procedure B. Solid (0.84 g, 100%) that was used without further purification. ^{1}H NMR (DMSO-d_6): δ 0.78 (3H, t, J = 7.4 Hz), 1.34 (2H, m), 2.60 (2H, t, J = 7.0 Hz), 5.87 (2H, s), 6.60 (2H, d, J = 8.7 Hz), 7.03 (1H, s), 7.40 (2H, d, J = 8.7 Hz).

*4.6.4.33. 4-Amino-N-isobutylbenzenesulfonamide (**14p**).* From **13p** (0.81 g, 3.1 mmol) with general procedure B. Yellow solid (0.61 g, 86%) that was used without further purification. ^{1}H NMR (DMSO-d_6): δ 0.79 (6H, d, J = 6.6 Hz), 1.59 (1H, m), 2.44 (2H, t, J = 6.5 Hz), 5.87 (2H, s), 6.59 (2H, d, J = 8.7 Hz), 7.06 (1H, t, J = 6.1 Hz), 7.40 (2H, d, J = 8.7 Hz).

*4.6.4.34. N,N-diallyl-4-aminobenzenesulfonamide (**14q**).* From **13q** (0.98 g, 3.5 mmol) with general procedure B. Yellow solid (0.87 g, 99%) that was used without further purification. ^{1}H NMR (DMSO-d_6): δ 3.64 (4H, d, J = 6.1 Hz), 5.12 (2H, dq, J = 10.3, 1.4 Hz), 5.16 (2H, dq, J = 17.1, 1.6 Hz), 5.61 (2H, ddt, J = 17.1, 10.3, 6.2 Hz), 6.01 (2H, s), 6.62 (2H, d, J = 8.7 Hz), 7.42 (2H, d, J = 8.7 Hz).

*4.6.4.35. N-((4-(N,N-diallylsulfamoyl)phenyl)carbamothioyl)-[1,1′-biphenyl]-4-carboxamide (**1**).* From **14q** (0.23 g, 0.9 mmol) with general procedure C. Light yellow solid (0.22 g, 49%). ^{1}H NMR (DMSO-d_6): δ 3.78 (4H, d, J = 6.3 Hz), 5.15 (1H, dq, J = 10.3, 1.4 Hz), 5.19 (1H, dq, J = 17.1, 1.4 Hz), 5.63 (1H, ddt, J = 17.1, 10.3, 6.2 Hz), 7.45 (1H, t, J = 7.7 Hz), 7.53 (2H, t, J = 7.7 Hz), 7.78 (2H, d, J = 7.4 Hz), 7.87 (4H, m), 8.03 (2H, d, J = 8.7 Hz), 8.10 (2H, d, J = 8.3 Hz), 11.75 (1H, s), 12.81 (1H, s); ^{13}C NMR (DMSO-d_6): δ 49.4, 118.8, 124.1, 126.6, 127.0, 127.7, 128.5, 129.1, 129.5, 130.8, 132.8, 136.4, 138.7, 141.9, 144.6, 167.8, 179.1; ESI-MS 490.00 $[M-H]^-$; Anal. Calcd for $C_{26}H_{25}N_3O_3S_2 \times 0.3H_2O$: C 62.83, N 8.45, H 5.19, S 12.90; found: C 62.40, N 8.41, H 4.80, S 12.95. Purity (≥95%) was also determined by HPLC. Eluent: acetate buffer pH 5/acetonitrile (40:60).

*4.6.4.36. N-((4-(N-Benzylsulfamoyl)phenyl)carbamothioyl)-[1,1′-biphenyl]-4-carboxamide (**17a**).* From **14a** (0.20 g, 0.8 mmol) with general procedure C. Light yellow solid (100%). ^{1}H NMR (DMSO-d_6): δ 4.02 (2H, d, J = 6.4 Hz), 7.20–7.33 (5H, m), 7.45 (1H, t, J = 7.3 Hz), 7.52 (2H, t, J = 7.5 Hz), 7.78 (2H, d, J = 7.4 Hz), 7.84 (2H, d, J = 8.6 Hz), 7.86 (2H, d J = 8.3 Hz),7.98 (2H, d, J = 8.6 Hz), 8.11 (2H, d, J = 8.3 Hz), 8.18 (1H, t, J = 6.3 Hz), 11.75 (1H, s), 12.80 (1H, s); ^{13}C NMR (DMSO-d_6): δ 46.2, 124.3, 126.7, 127.1, 127.3, 127.7, 128.3, 128.6, 129.2, 129.6, 130.0, 130.8, 137.7, 137.9, 138.8, 141.5, 144.7, 167.9, 179.3; ESI-MS 499.98 $[M-H]^-$; Anal. Calcd for $C_{27}H_{23}N_3O_3S_2 \times 0.1$ hexane: C 64.97, N 8.24, H 4.82, S 12.57; found: C 65.08, N 7.79, H 4.99, S 11.72. Purity (≥95%) was also determined by HPLC. Eluent: acetate buffer pH 5/acetonitrile (40:60).

*4.6.4.37. N-((4-(N-(4-Fluorobenzyl)sulfamoyl)phenyl)carbamothioyl)-[1,1′-biphenyl]-4-carboxamide (**17b**).* From **14b** (0.35 g, 1.2 mmol) with general procedure C. Light yellow solid (40 mg, 6%). ^{1}H NMR (DMSO-d_6): δ 4.01 (2H, d, J = 6.2 Hz), 7.12 (2H, t, J = 8.8 Hz), 7.29 (2H, dd, J = 8.8, 5.5 Hz), 7.45 (1H, t, J = 7.3 Hz), 7.53 (2H, t, J = 7.5 Hz), 7.79 (2H, d, J = 7.4 Hz), 7.83 (2H, d, J = 8.6 Hz), 7.87 (2H, d, J = 8.8 Hz), 7.97 (2H, d, J = 8.8 Hz), 8.12 (2H, d, J = 8.6 Hz), 8.22 (1H, t, J = 6.3 Hz), 11.74 (1H, s), 12.77 (1H, s); ^{13}C NMR (DMSO-d_6): δ 45.4, 115.0 (d, $^2J_{CF}$ = 21.2 Hz), 124.3, 126.6, 127.0, 127.2, 128.5, 129.2, 129.4, 129.5 (d, $^3J_{CF}$ = 8.2 Hz), 130.8, 133.9 (d, $^4J_{CF}$ = 2.9 Hz), 137.8, 138.7, 141.4, 144.7, 161.3 (d, $^1J_{CF}$ = 242.5 Hz), 167.8, 179.3; ESI-MS 518.05 $[M-H]^-$; Anal. Calcd for $C_{27}H_{22}FN_3O_3S_2$: C 62.41, N 8.09, H 4.27, S 12.34; found: C 62.43, N 7.66, H 4.17, S 10.00.

*4.6.4.38. N-((4-(N-(4-Iodobenzyl)sulfamoyl)phenyl)carbamothioyl)-[1,1′-biphenyl]-4-carboxamide (**17c**).* From **14c** (0.29 g, 0.7 mmol) with general procedure C. Light yellow solid (60 mg, 13%). ^{1}H NMR

(DMSO-d_6): δ 3.98 (2H, d, J = 6.1 Hz), 7.06 (2H, d, J = 8.3 Hz), 7.45 (1H, t, J = 7.3 Hz), 7.55 (2H, t, J = 7.6 Hz), 7.65 (2H, d, J = 8.3 Hz), 7.78 (2H, d, J = 7.3 Hz), 7.82 (2H, d, J = 8.7 Hz), 7.87 (2H, d, J = 8.4 Hz), 7.96 (2H, d, J = 8.7 Hz), 8.11 (2H, d, J = 8.4 Hz), 8.20 (1H, br t, J = 6.2 Hz), 11.74 (1H, br s), 12.80 (1H, br s); ^{13}C NMR (DMSO-d_6): δ 45.6, 93.0, 124.2, 126.6, 127.0, 127.2, 128.5, 129.1, 129.5, 129.9, 130.8, 137.0, 137.6, 137.7, 138.7, 141.5, 144.6, 167.8, 179.3; ESI-MS 625.75 [M−H]$^-$; Anal. Calcd for $C_{27}H_{22}IN_3O_3S_2$: C 51.68, N 6.70, H 3.53, S 10.22; found: C 51.96, N 6.49, H 3.42, S 9.99.

*4.6.4.39. N-((4-(N-(4-Methylbenzyl)sulfamoyl)phenyl)carbamothioyl)-[1,1′-biphenyl]-4-carboxamide (**17d**).* From **14d** (0.40 g, 1.4 mmol) with general procedure C. White solid (60 mg, 8%). ^{1}H NMR (DMSO-d_6): δ 2.26 (3H, s), 3.97 (2H, d, J = 6.3 Hz), 7.11 (4H, m), 7.45 (1H, t, J = 7.4 Hz), 7.53 (2H, t, J = 7.8 Hz), 7.78 (2H, d, J = 7.4 Hz), 7.83 (2H, d, J = 8.7 Hz), 7.87 (2H, d, J = 8.7 Hz), 7.96 (2H, d, J = 8.8 Hz), 8.11 (2H, d, J = 8.7 Hz), 11.74 (1H, s), 12.79 (1H, s); ^{13}C NMR (DMSO-d_6): δ 20.7, 45.9, 124.2, 126.6, 127.0, 127.2, 127.6, 128.5, 128.8, 129.1, 129.5, 130.8, 134.5, 136.3, 137.8, 138.7, 141.4, 144.6, 167.8, 179.3; ESI-MS 513.96 [M−H]$^-$; Anal. Calcd for $C_{28}H_{25}N_3O_3S_2$: C 65.22, N 8.15, H 4.89, S 12.44; found: C 65.67, N 7.87, H 4.68, S 11.34.

*4.6.4.40. N-((4-(N-(4-Methoxybenzyl)sulfamoyl)phenyl)carbamothioyl)-[1,1′-biphenyl]-4-carboxamide (**17e**).* From **14e** (0.22 g, 0.8 mmol) with general procedure C. White solid (0.14 g, 35%). ^{1}H NMR (DMSO-d_6): δ 3.72 (3H, s), 3.95 (2H, d, J = 6.3 Hz), 6.84 (2H, d, J = 8.7 Hz), 7.15 (2H, d, J = 8.8 Hz), 7.45 (1H, t, J = 7.3 Hz), 7.53 (2H, t, J = 7.9 Hz), 7.78 (2H, d, J = 7.4 Hz), 7.83 (2H, d, J = 8.7 Hz), 7.87 (2H, d, J = 8.5 Hz), 7.96 (2H, d, J = 8.8 Hz), 8.08 (1H, t, J = 6.3 Hz), 8.11 (2H, d, J = 8.5 Hz), 11.74 (1H, s), 12.79 (1H, s); ^{13}C NMR (DMSO): δ 45.7, 55.0, 113.6, 124.2, 126.6, 127.0, 127.2, 128.5, 128.9, 129.1, 129.4, 129.5, 130.8, 137.8, 138.7, 141.3, 144.6, 158.4, 167.8, 179.3; ESI-MS 529.95 [M−H]$^-$; Anal. Calcd for $C_{28}H_{25}N_3O_4S_2$: C 63.26, N 7.90, H 4.74, S 12.06; found: C 62.89, N 7.87, H 4.36, S 12.48.

*4.6.4.41. N-((4-(Benzylcarbamoyl)phenyl)carbamothioyl)-[1,1′-biphenyl]-4-carboxamide (**17f**).* From **14f** (0.40 g, 1.8 mmol) with general procedure C. White solid (0.29 g, 35%). ^{1}H NMR (DMSO-d_6): δ 4.50 (2H, d, J = 6.2 Hz), 7.25 (1H, m), 7.34 (4H, m), 7.45 (1H, t, J = 7.5 Hz), 7.53 (2H, t, J = 7.6 Hz), 7.78 (2H, d, J = 7.3 Hz), 7.86 (4H, d, J = 8.5 Hz), 7.95 (2H, d, J = 8.5 Hz), 8.10 (2H, d, J = 8.5 Hz), 9.07 (1H, t, J = 6.1 Hz), 11.68 (1H, s), 12.77 (1H, s); ^{13}C NMR (DMSO-d_6): δ 42.6, 123.6, 126.6, 126.7, 127.0, 127.2, 127.8, 128.3, 128.5, 129.1, 129.5, 130.8, 131.8, 138.7, 139.7, 140.5, 144.6, 165.5, 167.9, 179.1; ESI-MS 466.12 [M+H]$^+$; Anal. Calcd for $C_{28}H_{23}N_3O_2S$: C 72.24, N 9.03, H 4.98, S 6.89; found: C 72.33, N 8.92, H 4.92, S 7.05.

*4.6.4.42. N-((4-(N-Phenylsulfamoyl)phenyl)carbamothioyl)-[1,1′-biphenyl]-4-carboxamide (**17g**).* From **14g** (0.22 g, 0.9 mmol) with general procedure C. Light yellow solid (40 mg, 9%). ^{1}H NMR (DMSO-d_6): δ 7.03 (1H, tt, J = 7.4. 1.1 Hz), 7.12 (2H, dd, J = 8.6, 1.1 Hz), 7.25 (2H, dd, J = 8.6, 7.5 Hz), 7.44 (1H, t, J = 7.3 Hz), 7.52 (2H, t, J = 7.6 Hz), 7.77 (2H, d, J = 7.2 Hz), 7.79 (2H, d, J = 8.8 Hz), 7.85 (2H, d, J = 8.4 Hz), 7.95 (2H, d, J = 8.8 Hz), 8.08 (2H, d, J = 8.4 Hz), 10.30 (1H, s), 11.70 (1H, s), 12.74 (1H, s); ^{13}C NMR (DMSO-d_6): δ 120.0, 124.1, 126.6, 127.0, 127.4, 128.5, 129.1, 129.2, 129.5(x2C), 130.7, 136.4, 137.6, 138.7, 141.9, 144.6, 167.7, 179.2; ESI-MS 485.99 [M−H]$^-$; Anal. Calcd for $C_{26}H_{21}N_3O_3S_2 \times 0.15H_2O$: C 63.69, N 8.57, H 4.38, S 13.08; found: C 63.28, N 8.39, H 4.45, S 12.45.

*4.6.4.43. N-((4-(N-(4-Chlorophenyl)sulfamoyl)phenyl)carbamothioyl)-[1,1′-biphenyl]-4-carboxamide (**17h**).* From **14h** (0.62 g, 2.2 mmol) with general procedure C. White solid (0.55 g, 48%). ^{1}H NMR (DMSO-d_6): δ 7.14 (2H, d, J = 8.8 Hz), 7.33 (2H, d, J = 8.8 Hz), 7.45 (1H, t, J = 7.6 Hz), 7.53 (2H, t, J = 7.3 Hz), 7.78 (2H, m), 7.80 (2H, d, J = 8.8 Hz), 7.86 (2H, d, J = 8.8 Hz), 7.98 (2H, d, J = 8.8 Hz), 8.09 (2H, d, J = 8.8 Hz), 10.47 (1H, s), 11.72 (1H, s), 12.76 (1H, s); ^{13}C NMR (DMSO-d_6): δ 121.6, 124.2, 126.6, 127.0, 127.4, 128.2, 128.5, 129.1, 129.2, 129.5, 130.7, 136.0, 136.6, 138.7, 142.0, 144.6, 167.7, 179.2; ESI-MS 519.95 [M−H]$^-$; Anal. Calcd for $C_{26}H_{20}ClN_3O_3S_2 \times 0.3H_2O$: C 59.21, N 7.97, H 3.94, S 12.16; found: C 58.82, N 7.88, H 3.85, S 12.04.

*4.6.4.44. N-((4-(N-(4-butylphenyl)sulfamoyl)phenyl)carbamothioyl)-[1,1′-biphenyl]-4-carboxamide (**17i**).* From **14i** (0.75 g, 2.5 mmol) with general procedure C. Light yellow solid (0.36 g, 27%). ^{1}H NMR (DMSO-d_6): δ 0.86 (3H, t, J = 7.4 Hz), 1.24 (2H, sxt, J = 7.6 Hz), 1.47 (2H, m), 2.46 (2H, t, J = 7.6 Hz), 7.01 (2H, d, J = 8.5 Hz), 7.06 (2H, d, J = 8.2 Hz), 7.44 (1H, t, J = 7.3 Hz), 7.52 (2H, t, J = 7.3 Hz), 7.77 (4H, m), 7.85 (2H, d, J = 8.5 Hz), 7.94 (2H, d, J = 8.7 Hz), 8.09 (2H, d, J = 8.5 Hz), 10.16 (1H, s), 11.71 (1H, s), 12.75 (1H, s); ^{13}C NMR (DMSO-d_6): δ 13.7, 21.7, 33.0, 34.1, 120.5, 124.0, 126.6, 127.0, 127.4, 128.5, 128.9, 129.1, 129.5, 130.7, 135.1, 136.5, 138.3, 138.7, 141.8, 144.6, 167.7, 179.2; ESI-MS 541.98 [M−H]$^-$; Anal. Calcd for $C_{30}H_{29}N_3O_3S_2$: C 66.27, N 7.73, H 5.38, S 11.79; found: C 65.94, N 7.98, H 5.43, S 11.28.

*4.6.4.45. N-((4-(N-Phenethylsulfamoyl)phenyl)carbamothioyl)-[1,1′-biphenyl]-4-carboxamide (**17j**).* From **14j** (0.39 g, 1.4 mmol) with general procedure C. White solid (0.07 g, 10%). ^{1}H NMR (DMSO-d_6): δ 2.70 (2H, t, J = 7.4 Hz), 3.00 (2H, dt, J = 7.6, 5.3 Hz), 7.16–7.22 (3H, m), 7.28 (2H, t, J = 7.3 Hz), 7.45 (1H, t, J = 7.6 Hz), 7.53 (2H, t, J = 7.6 Hz), 7.75–7.80 (3H, m), 7.82 (2H, d, J = 8.8 Hz), 7.87 (2H, d, J = 8.5 Hz), 7.97 (2H, d, J = 8.5 Hz), 8.11 (2H, d, J = 8.5 Hz), 11.76 (1H, s), 12.79 (1H, s); ^{13}C NMR (DMSO-d_6): δ 35.3, 44.1, 124.3, 126.2, 126.6, 127.0, 127.1, 128.3, 128.4, 128.7, 129.1, 129.5, 130.8, 137.4, 138.7, 141.4, 144.6, 167.8, 179.3; ESI-MS 514.09 [M−H]$^-$; Anal. Calcd for $C_{28}H_{25}N_3O_3S_2$: C 65.22, N 8.15, H 4.89, S 12.44; found: C 65.14, N 8.22, H 5.02, S 10.91.

*4.6.4.46. N-((4-(Phenethylcarbamoyl)phenyl)carbamothioyl)-[1,1′-biphenyl]-4-carboxamide (**17k**).* From **14k** (0.40 g, 1.7 mmol) with general procedure C. Light yellow solid (0.04 g, 8%). ^{1}H NMR (DMSO-d_6): δ 2.86 (2H, t, J = 7.5 Hz), 3.50 (2H, dt, J = 7.9, 6.5), 7.21 (1H, t, J = 7.5 Hz), 7.24–7.34 (4H, m), 7.45 (1H, t, J = 7.4 Hz), 7.53 (2H, t, J = 7.6 Hz), 7.78 (2H, d, J = 7.4 Hz), 7.84–7.89 (2H, m), 8.97 (2H, d, J = 8.4 Hz), 8.02 (2H, d, J = 8.6 Hz), 8.10 (2H, d, J = 8.4 Hz), 8.59 (1H, t, J = 5.5 Hz), 11.68 (1H, s), 12.76 (1H, s); ^{13}C NMR (DMSO-d_6): δ 35.1, 40.9, 123.5, 126.1, 126.6, 127.0, 127.6, 128.3, 128.5, 128.6, 129.1, 129.5, 130.8, 132.1, 138.7, 139.5, 140.4, 144.6, 165.4, 167.9, 179.0; ESI-MS 478.02 [M−H]$^-$; Anal. Calcd for $C_{29}H_{25}N_3O_2S \times 0.2H_2O$: C 72.09, N 8.70, H 5.30, S 6.64; found: C 71.65, N 8.74, H 4.97, S 6.19.

*4.6.4.47. N-((4-(N-(Furan-2-ylmethyl)sulfamoyl)phenyl)carbamothioyl)-[1,1′-biphenyl]-4-carboxamide (**17l**).* From **14l** (0.41 g, 1.6 mmol) with general procedure C. Light yellow solid (0.09 g, 11%). ^{1}H NMR (DMSO-d_6): δ 4.04 (2H, d, J = 6.0 Hz), 6.20 (1H, d, J = 3.4 Hz), 6.32 (1H, dd, J = 3.4, 1.6 Hz), 7.45 (1H, t, J = 7.4 Hz), 7.53 (2H, t, J = 7.7 Hz), 7.77–7.82 (m, 3H), 7.84 (2H, d, J = 8.4 Hz), 7.87 (2H, d, J = 8.4 Hz), 7.95 (2H, d, J = 8.5 Hz), 8.11 (2H, d, J = 8.5 Hz), 8.22 (1H, t, J = 6.3 Hz), 11.78 (1H, s), 12.79 (1H, s). ^{13}C NMR (DMSO-d_6): δ ~41 (overlap with the solvent), 108.0, 110.4, 124.1, 126.6, 127.0, 127.1, 128.5, 129.1, 129.5, 130.8, 137.7, 138.7, 141.3, 142.5, 144.6, 150.5, 167.8, 179.3; ESI-MS 492.02 [M+H]$^+$; Anal. Calcd for $C_{25}H_{21}N_3O_4S_2$: C 61.92, N 8.23, H 4.75, S 12.56; found: C 62.32, N 8.36, H 4.45, S 12.58. Purity (≥95%) was also determined by HPLC. Eluent: water/acetonitrile (40:60).

*4.6.4.48. N-((4-(N-(2-(1H-Indol-3-yl)ethyl)sulfamoyl)phenyl)carbamothioyl)-[1,1′-biphenyl]-4-carboxamide (**17m**).* From **14m** (0.43 g,

1.4 mmol) with general procedure C. White solid (0.02 g, 3%). ^{1}H NMR (DMSO-d_6): δ 2.81 (2H, t, J = 7.6 Hz), 3.05 (2H, dt, J = 7.8, 5.6 Hz)), 6.96 (1H, ddd, J = 7.9, 7.0, 1.0 Hz), 7.05 (1H, ddd, J = 8.1, 7.0, 1.1 Hz), 7.12 (1H, d, J = 2.6 Hz), 7.32 (1H, d, J = 8.1 Hz), 7.40 (1H, d, J = 7.9 Hz), 7.45 (1H, t, J = 7.4 Hz), 7.53 (2H, t, J = 7.6 Hz), 7.77 (3H, m), 7.82 (2H, d, J = 8.8 Hz), 7.86 (2H, d, J = 8.5 Hz), 7.94 (2H, d, J = 8.8 Hz), 8.10 (2H, d, J = 8.5 Hz), 10.81 (1H, s), 11.73 (1H, s), 12.77 (1H, s); ^{13}C NMR (DMSO-d_6): δ 25.4, 43.5, 110.9, 111.4, 118.0, 118.3, 120.9, 123.0, 124.3, 126.6, 126.9, 127.0, 127.1, 128.5, 129.1, 129.5, 130.7, 136.1, 137.7, 138.7, 141.3, 144.6, 167.8, 179.3; ESI-MS 552.93 [M−H]$^-$; Anal. Calcd for $C_{30}H_{26}N_4O_3S_2$: C 64.96, N 10.10, H 4.72, S 11.56; found: C 64.69, N 9.68, H 4.50, S 10.62.

*4.6.4.49. N-((4-(N-Allylsulfamoyl)phenyl)carbamothioyl)-[1,1′-biphenyl]-4-carboxamide (**17n**).* From **14n** (0.30 g, 1.4 mmol) with general procedure C. White solid (0.13 g, 20%). ^{1}H NMR (DMSO): δ 3.45 (2H, br t, J = 5.7 Hz), 5.04 (1H, dq, J = 10.3, 1.5 Hz), 5.17 (1H, dq, J = 17.2, 1.6 Hz), 5.70 (1H, ddt, J = 17.2, 10.2, 5.7 Hz), 7.45 (1H, t, J = 7.5 Hz), 7.52 (2H, t, J = 7.6 Hz), 7.78 (2H, d, J = 7.3 Hz), 7.82 (1H, m), 7.83 (2H, d, J = 8.8 Hz), 7.86 (2H,d, J = 8.6 Hz), 7.99 (2H, d, J = 8.8 Hz), 8.10 (2H, d, J = 8.5 Hz), 11.74 (1H, s), 12.79 (1H, s); ^{13}C NMR (DMSO-d_6): δ 45.0, 116.6, 124.2, 126.6, 127.0, 127.2, 128.5, 129.1, 129.5, 130.7, 134.1, 137.7, 138.7, 141.4, 144.6, 167.8, 179.3; ESI-MS 449.97 [M−H]$^-$; Anal. Calcd for $C_{23}H_{21}N_3O_3S_2$: C 61.18, N 9.31, H 4.69, S 14.20; found: C 61.17, N 9.25, H 4.24, S 14.50.

*4.6.4.50. N-((4-(N-Propylsulfamoyl)phenyl)carbamothioyl)-[1,1′-biphenyl]-4-carboxamide (**17o**).* From **14o** (0.11 g, 0.5 mmol) with general procedure C. Light yellow solid (0.09 g, 38%). ^{1}H NMR (DMSO-d_6): δ 0.81 (3H, t, J = 7.3 Hz), 1.39 (2H, m), 2.73 (2H, m), 7.45 (1H, t, J = 7.3 Hz), 7.53 (2H, t, J = 7.5 Hz), 7.60 (1H, t, J = 5.8 Hz), 7.78 (2H, d, J = 7.4 Hz), 7.82 (2H, d, J = 8.5 Hz), 7.86 (2H, d, J = 8.5 Hz), 7.98 (2H, d, J = 8.4 Hz), 8.10 (2H, d, J = 8.4 Hz), 11.73 (1H, s), 12.78 (1H, s); ^{13}C NMR (DMSO-d_6): δ 11.1, 22.4, 44.4, 124.3, 126.6, 127.0, 127.1, 128.5, 129.1, 129.5, 130.8, 137.7, 138.7, 141.3, 144.6, 167.8, 179.3; ESI-MS 452.00 [M−H]$^-$; Anal. Calcd for $C_{23}H_{23}N_3O_3S_2$: C 60.90, N 9.26, H 5.11, S 14.14; found: C 60.83, N 9.29, H 5.27, S 13.33.

*4.6.4.51. N-((4-(N-Isobutylsulfamoyl)phenyl)carbamothioyl)-[1,1′-biphenyl]-4-carboxamide (**17p**).* From **14p** (0.15 g, 0.6 mmol) with general procedure C. Light yellow solid (0.05 g, 16%). ^{1}H NMR (DMSO-d_6): δ 0.83 (6H, d, J = 6.7 Hz), 1.64 (1H, h, J = 6.7 Hz), 2.58 (2H, t, J = 6.4 Hz), 7.45 (1H, t, J = 7.4 Hz), 7.52 (2H, t, J = 7.6 Hz), 7.63 (1H, t, J = 6.2 Hz), 7.78 (2H, d, J = 7.4 Hz), 7.83 (2H, d, J = 8.8 Hz), 7.86 (2H, d, J = 8.4), 7.98 (2H, d, J = 8.8 Hz), 8.10 (2H, d, J = 8.4 Hz), 11.73 (1H, s), 12.79 (1H, s); ^{13}C NMR (DMSO-d_6): δ 19.9, 28.1, 50.0, 124.2, 126.6, 127.0, 127.1, 128.5, 129.1, 129.5, 130.7, 137.8, 138.7, 141.3, 144.6, 167.8, 179.3; ESI-MS 466.01 [M−H]$^-$; Anal. Calcd for $C_{24}H_{25}N_3O_3S_2$ × 0.05 hexane: C 61.85, N 8.90, H 5.49, S 13.59; found: C 62.29, N 8.64, H 5.70, S 11.91. Purity (≥95%) was also determined by HPLC. Eluent: acetate buffer pH 5/MeOH (40:60).

4.7. In vitro studies

4.7.1. GPR55

PathHunter eXpress GPR55 CHO−K1 β-arrestin GPCR assay was used to screen the compounds' ability to activate GPR55 at 10 μM concentrations. The assay kits were purchased from DiscoveRx (catalog no. 93-0245E2CP0M). The screening was done according the protocol provided with the kits. The luminescence was measured using a Victor2 plate reader (PerkinElmer). Results are reported as a percentage of the luminescence given by the reference compound LPI (L-α-lysophosphatidylinositol, liver, bovine-sodium salt, Avanti Polar Lipids, Inc.) at 1 μM concentration (mean with range of two experiments performed in duplicate). Compounds having an intact biphenyl carboxamide moiety and a promising screening result (>100%) were further evaluated using a HEK-293 AD cell line stably expressing human GPR55. Compounds **17f** and **17k** were also tested with the HEK cell line as a comparison (screening results 67% and 68%, respectively). Effects on calcium signalling were determined using single cell, fura 2-based, digital epifluorescence microscopy [29]. Cells were cultured on poly-L-lysine coated glass coverslips and were serum-starved overnight prior to experimental studies. Compounds were applied by bath perfusion in a standard HEPES-buffered saline at 30–32 °C. Ratiometric images (350/380 nm) were obtained every 5 s and changes in intracellular calcium levels are represented a change in the fura 2 fluorescence ratio. Mean peak responses were determined from 24 cells, derived from two separate experiments (12 cells from each, selected at random) for each agonist concentration and the results are reported as EC_{50} values. In these studies 1-arachidonoyl-2-hydroxy-*sn*-glycero-3-phosphoinositol (ARA-LPI) (Avanti Polar Lipids, Inc. Alabaster, AL, USA) was used as a reference agonist.

4.7.2. CB1R and CB2R

All compounds were tested for their CB1 and CB2 receptor activities by using the [^{35}S]GTPγS binding assay according to procedures described in literature [50,51].

4.7.3. FAAH

Inhibitory activity of the synthesized compounds was determined using membranes of hFAAH overexpressing COS-7 cells as described previously [52]. The final incubation volume (100 μl) contained 1 μg of protein and the substrate concentration was 20 μM [10 nM of *N*-[^{3}H]arachidonoylethanolamine (^{3}H-AEA) having specific activity of 60 Ci/mmol and concentration of 1 mCi/ml].

4.7.4. MGL

Inhibitory activity of the synthesized compounds was determined using lysates of hMGL overexpressing HEK cells as described previously [53]. The final incubation volume (100 μl) contained 2.5 μg of protein and the substrate concentration was 50 μM.

4.7.5. ABHD6 and ABHD12

Glycerol liberated from 2-AG hydrolysis was determined with a sensitive fluorescent glycerol assay using lysates of HEK293 cells with transient overexpression of hABHD6 or hABHD12 as previously described [54]. In this approach, glycerol production was coupled via a three-step enzymatic cascade to hydrogen peroxide (H_2O_2) dependent generation of resorufin whose fluorescence (λ_{ex} 530; λ_{em} 590 nm) was kinetically monitored using a Tecan Infinite M200 plate reader (Tecan Group Ltd., Männedorf, Switzerland). Briefly, lysates of hABHD6 or hABHD12 overexpressing HEK293 cells (99 μl, 0.3 μg protein/well) were pretreated for 30 min with the solvent (DMSO) or the indicated concentrations of the inhibitors (1 μl), after which 2-AG (100 μl, 12.5 μM final concentration) was added and the reaction kinetically monitored for 90 min. The assays routinely contained 0.5% (w/v) BSA (essentially fatty acid free) as a carrier.

Acknowledgements

This work was supported by the Academy of Finland (decision nos. 128056, 127653 and 139620), Biocenter Finland/DDCB, the National Graduate School of Organic Chemistry and Chemical Biology, and the Carnegie Trust (Scotland). The authors are grateful to Tiina Koivunen, Miia Reponen, Satu Marttila, and Helly Rissanen for technical assistance. The molecular modelling part was developed using the equipment purchased within the project "The equipment of innovative laboratories doing research on new

medicines used in the therapy of civilization and neoplastic diseases" within the Operational Program Development of Eastern Poland 2007–2013, Priority Axis I modern Economy, operations I.3 Innovation promotion. The research was partially performed during the postdoctoral fellowship of Agnieszka A. Kaczor at University of Eastern Finland, Kuopio, Finland under Marie Curie fellowship. Calculations were partially performed under a computational grant by Interdisciplinary Center for Mathematical and Computational Modeling (ICM), Warsaw, Poland, grant number G30-18 and under resources and licenses from CSC, Finland.

Appendix A. Supplementary data

Supplementary data related to this article can be found at http://dx.doi.org/10.1016/j.ejmech.2015.10.050.

References

[1] R.A. Ross, The enigmatic pharmacology of GPR55, Trends Pharmacol. Sci. 30 (3) (2009) 156–163.
[2] S. Oka, K. Nakajima, A. Yamashita, S. Kishimoto, T. Sugiura, Identification of GPR55 as a lysophosphatidylinositol receptor, Biochem. Biophys. Res. Commun. 362 (4) (2007) 928–934.
[3] S. Oka, T. Toshida, K. Maruyama, K. Nakajima, A. Yamashita, T. Sugiura, 2-Arachidonoyl-sn-glycero-3-phosphoinositol: a possible natural ligand for GPR55, J. Biochem. 145 (1) (2009) 13–20.
[4] A. Kapur, P. Zhao, H. Sharir, Y. Bai, M.G. Caron, L.S. Barak, M.E. Abood, Atypical responsiveness of the orphan receptor GPR55 to cannabinoid ligands, J. Biol. Chem. 284 (43) (2009) 29817–29827.
[5] P. Zhao, M.E. Abood, GPR55 and GPR35 and their relationship to cannabinoid and lysophospholipid receptors, Life Sci. 92 (8–9) (2013) 453–457.
[6] A. Moriconi, I. Cerbara, M. Maccarrone, A. Topai, GPR55: current knowledge and future perspectives of a purported "type-3" cannabinoid receptor, Curr. Med. Chem. 17 (14) (2010) 1411–1429.
[7] P.C. Staton, J.P. Hatcher, D.J. Walker, A.D. Morrison, E.M. Shapland, J.P. Hughes, E. Chong, P.K. Mander, P.J. Green, A. Billinton, M. Fulleylove, H.C. Lancaster, J.C. Smith, L.T. Bailey, A. Wise, A.J. Brown, J.C. Richardson, I.P. Chessell, The putative cannabinoid receptor GPR55 plays a role in mechanical hyperalgesia associated with inflammatory and neuropathic pain, Pain 139 (1) (2008) 225–236.
[8] N.A. Balenga, E. Aflaki, J. Kargl, W. Platzer, R. Schröder, S. Blättermann, E. Kostenis, A.J. Brown, A. Heinemann, M. Waldhoer, GPR55 regulates cannabinoid 2 receptor-mediated responses in human neutrophils, Cell Res. 21 (10) (2011) 1452–1469.
[9] M. Pietr, E. Kozela, R. Levy, N. Rimmerman, Y.H. Lin, N. Stella, Z. Vogel, A. Juknat, Differential changes in GPR55 during microglial cell activation, FEBS Lett. 583 (2009) 2071–2076.
[10] S. Sylantyev, T.P. Jensen, R.A. Ross, D.A. Rusakov, Cannabinoid- and lysophosphatidylinositol-sensitive receptor GPR55 boosts neurotransmitter release at central synapses, Proc. Natl. Acad. Sci. U. S. A. 110 (13) (2013) 5193–5198.
[11] L.S. Whyte, E. Ryberg, N.A. Sims, S.A. Ridge, K. Mackie, P.J. Greasley, R.A. Ross, M.J. Rogers, The putative cannabinoid receptor GPR55 affects osteoclast function in vitro and bone mass in vivo, PNAS 106 (38) (2009) 16511–16516.
[12] L.A. Ford, A.J. Roelofs, S. Anavi-Goffer, L. Mowat, D.G. Simpson, A.J. Irving, M.J. Rogers, A.M. Rajnicek, R.A. Ross, A role for L-alpha-lysophosphatidylinositol and GPR55 in the modulation of migration, orientation and polarization of human breast cancer cells, Br. J. Pharmacol. 160 (3) (2010) 762–771.
[13] C. Andradas, M.M. Caffarel, E. Pérez-Gómez, M. Salazar, M. Lorente, G. Velasco, M. Guzmán, C. Sánchez, The orphan G protein-coupled receptor GPR55 promotes cancer cell proliferation via ERK, Oncogene 30 (2) (2011) 245–252.
[14] R. Piñeiro, T. Maffucci, M. Falasca, The putative cannabinoid receptor GPR55 defines a novel autocrine loop in cancer cell proliferation, Oncogene 30 (2) (2011) 142–152.
[15] L. Huang, J.C. Ramirez, G.A. Frampton, L.E. Golden, M.A. Quinn, H.Y. Pae, D. Horvat, L.J. Liang, S. DeMorrow, Anandamide exerts its antiproliferative actions on cholangiocarcinoma by activation of the GPR55 receptor, Lab. Invest 91 (7) (2011) 1007–1017.
[16] R. Schicho, M. Storr, A potential role for GPR55 in gastrointestinal functions, Curr. Opin. Pharmacol. 12 (6) (2012) 653–658.
[17] J.M. Moreno-Navarrete, V. Catalán, L. Whyte, A. Díaz-Arteaga, R. Vázquez-Martínez, F. Rotellar, R. Guzmán, J. Gómez-Ambrosi, M.R. Pulido, W.R. Russell, M. Imbernón, R.A. Ross, M.M. Malagón, C. Dieguez, J.M. Fernández-Real, G. Frühbeck, R. Nogueiras, The L-α-lysophosphatidylinositol/GPR55 system and its potential role in human obesity, Diabetes 61 (2) (2012) 281–291.
[18] H. Ishiguro, E.S. Onaivi, Y. Horiuchi, K. Imai, G. Komaki, T. Ishikawa, M. Suzuki, Y. Watanabe, T. Ando, S. Higuchi, T. Arinami, Functional polymorphism in the GPR55 gene is associated with anorexia nervosa, Synapse 65 (2) (2011) 103–108.
[19] A. Bondarenko, M. Waldeck-Weiermair, S. Naghdi, M. Poteser, R. Malli, W.F. Graier, GPR55-dependent and -independent ion signalling in response to lysophosphatidylinositol in endothelial cells, Br. J. Pharmacol. 161 (2) (2010) 308–320.
[20] S. Heynen-Genel, R. Dahl, S. Shi, L. Milan, S. Hariharan, Y. Bravo, E. Sergienko, M. Hedrick, S. Dad, D. Stonich, Y. Su, M. Vicchiarelli, A. Mangravita-Novo, L.H. Smith, T.D.Y. Chung, H. Sharir, L.S. Barak, M.E. Abood, Screening for selective ligands for GPR55-agonists [Updated 2011 May 26], in: Probe Reports from the NIH Molecular Libraries Program [Internet]. Bethesda (MD), National Center for Biotechnology Information, US, 2010. Available from: http://www.ncbi.nlm.nih.gov/books/NBK66152/.
[21] National Center for Biotechnology Information. PubChem BioAssay Database; AID=1961, Source: Burnham Center for Chemical Genomics (BCCG-a221-GPR55-agonist-assay), http://pubchem.ncbi.nlm.nih.gov/assay/assay.cgi?aid=1961 (accessed 10.04.13.).
[22] E. Kotsikorou, K.E. Madrigal, D.P. Hurst, H. Sharir, D.L. Lynch, S. Heynen-Genel, L.B. Milan, T.D. Chung, H.H. Seltzman, Y. Bai, M.G. Caron, L. Barak, M.E. Abood, P.H. Reggio, Identification of the GPR55 agonist binding site using a novel set of high-potency GPR55 selective ligands, Biochemistry 50 (25) (2011) 5633–5647.
[23] A.J. Brown, D.A. Daniels, M. Kassim, S. Brown, C.P. Haslam, V.R. Terrell, J. Brown, P.L. Nichols, P.C. Staton, A. Wise, S.J. Dowell, Pharmacology of GPR55 in yeast and identification of GSK494581A as a mixed-activity glycine transporter subtype 1 inhibitor and GPR55 agonist, J. Pharmacol. Exp. Ther. 337 (1) (2011) 236–246.
[24] J. Kargl, A.J. Brown, L. Andersen, G. Dorn, R. Schicho, M. Waldhoer, A. Heinemann, A selective antagonist reveals a potential role of g protein-coupled receptor 55 in platelet and endothelial cell function, J. Pharmacol. Exp. Ther. 346 (1) (2013) 54–66.
[25] S. Heynen-Genel, R. Dahl, S. Shi, L. Milan, S. Hariharan, E. Sergienko, M. Hedrick, S. Dad, D. Stonich, Y. Su, M. Vicchiarelli, A. Mangravita-Novo, L.H. Smith, T.D.Y. Chung, H. Sharir, M.G. Caron, L.S. Barak, M.E. Abood, Screening for Selective Ligands for GPR55-antagonists. Probe Reports from the NIH Molecular Libraries Program [Internet], National Center for Biotechnology Information (US), Bethesda (MD), 2010.
[26] E. Kotsikorou, H. Sharir, D.M. Shore, D.P. Hurst, D.L. Lynch, K.E. Madrigal, S. Heynen-Genel, L.B. Milan, T.D. Chung, H.H. Seltzman, Y. Bai, M.G. Caron, L.S. Barak, M.P. Croatt, M.E. Abood, P.H. Reggio, Identification of the GPR55 antagonist binding site using a novel set of high-potency GPR55 selective ligands, Biochemistry 52 (52) (2013) 9456–9469.
[27] V. Rempel, N. Volz, F. Gläser, M. Nieger, S. Bräse, C.E. Müller, Antagonists for the orphan G-protein-coupled receptor GPR55 based on a coumarin scaffold, J. Med. Chem. 56 (11) (2013) 4798–4810.
[28] V. Rempel, A. Fuchs, S. Hinz, T. Karcz, M. Lehr, U. Koetter, C.E. Müller, Magnolia extract, magnolol, and metabolites: activation of cannabinoid CB2 receptors and blockade of the related GPR55, ACS Med. Chem. Lett. 4 (1) (2013) 41–45.
[29] C.M. Henstridge, N.A. Balenga, L.A. Ford, R.A. Ross, M. Waldhoer, A.J. Irving, The GPR55 ligand L-alpha-lysophosphatidylinositol promotes RhoA-dependent Ca^{2+} signaling and NFAT activation, FASEB J. 23 (1) (2009) 183–193.
[30] A. Le Pera, A. Leggio, A. Liguori, Highly specific N-monomethylation of primary aromatic amines, Tetrahedron 62 (25) (2006) 6100–6106.
[31] M. Kapischke, T. Fischer, K. Tiessen, H. Tschesche, H.P. Bruch, H. Kalthoff, M.L. Kruse, Characterisation of a novel matrix metalloproteinase inhibitor on pancreatic adenocarcinoma cells in vitro and in an orthotopic pancreatic cancer model in vivo, Int. J. Oncol. 32 (1) (2008) 273–282.
[32] K. Namba, X. Zheng, K. Motoshima, H. Kobayashi, A. Tai, E. Takahashi, K. Sasaki, K. Okamoto, H. Kakuta, Design and synthesis of benzenesulfonanilides active against methicillin-resistant Staphylococcus aureus and vancomycin-resistant Enterococcus, Bioorg. Med. Chem. 16 (11) (2008) 6131–6144.
[33] C.K. Özer, H. Arslan, D. VanDerveer, N. Külcü, Synthesis and characterization of N-(arylcarbamothioyl)-cyclohexanecarboxamide derivatives: the crystal structure of N-(naphthalen-1-ylcarbamothioyl)cyclohexanecarboxamide, Molecules 14 (2) (2009) 655–666.
[34] M.K. Rauf, Imtiaz-ud-Din, A. Badshah, M. Gielen, M. Ebihara, D.D. Vos, S. Ahmed, Synthesis, structural characterization and in vitro cytotoxicity and anti-bacterial activity of some copper(I) complexes with N,N′-disubstituted thioureas, J. Inorg. Biochem. 103 (8) (2009) 1135–1144.
[35] M.N.S. Rad, A. Khalafi-Nezhad, Z. Asrari, S. Behrouz, Z. Amini, M. Behrouz, One-pot synthesis of sulfonamides from primary and secondary amine derived sulfonate salts using cyanuric chloride, Synthesis 23 (2009) 3983–3988.
[36] SYBYL-X 2.1, Tripos International, St. Louis, MO, 2011.
[37] Schrödinger Suite 2014-1, Induced Fit Docking Protocol; Glide Version 6.2, Prime Version 3.5, Schrödinger, LLC, New York, NY, 2014.
[38] Molecular Operating Environment (MOE) software, http://www.chemcomp.com/software.htm.
[39] S.G. Rasmussen, B.T. DeVree, Y. Zou, A.C. Kruse, K.Y. Chung, T.S. Kobilka, F.S. Thian, P.S. Chae, E. Pardon, D. Calinski, J.M. Mathiesen, S.T. Shah, J.A. Lyons, M. Caffrey, S.H. Gellman, J. Steyaert, G. Skiniotis, W.I. Weis, R.K. Sunahara, B.K. Kobilka, Crystal structure of the β2 adrenergic receptor-Gs protein complex, Nature 477 (2011) 549–555.
[40] N. Eswar, M.A. Marti-Renom, B. Webb, M.S. Madhusudhan, D. Eramian, M. Shen, U. Pieper, A. Sali, Comparative protein structure modeling with MODELLER, in: Current Protocols in Bioinformatics, John Wiley & Sons, Inc.,

2006. Supplement 15, 5.6.1-5.6.30.
[41] M.Y. Shen, A. Sali, Statistical potential for assessment and prediction of protein structures, Protein Sci. 15 (2006) 2507–2524.
[42] F. Melo, E. Feytmans, E. Assessing protein structures with a non-local atomic interaction energy, J. Mol. Biol. 277 (1998) 1141–1152.
[43] J.U. Bowie, R. Lüthy, D.A. Eisenberg, A method to identify protein sequences that fold into a known three-dimensional structure, Science 253 (1991) 164–170.
[44] R.A. Laskowski, M.W. MacArthur, D.S. Moss, J.M. Thornton, PROCHECK – a program to check the stereochemical quality of protein structures, J. App. Cryst. 26 (1993) 283–291.
[45] The PyMOL Molecular Graphics System, Version 1.5.0.3, Schrödinger, LLC.
[46] N. Guex, M.C. Peitsch, SWISS-MODEL and the Swiss-PdbViewer: an environment for comparative protein modeling, Electrophoresis 18 (1997) 2714–2723.
[47] Schrödinger Release 2014-1, Jaguar, Version 8.3, Schrödinger, LLC, New York, NY, 2014.
[48] Schrödinger Suite 2014-1, Protein Preparation Wizard; Epik Version 2.7, Impact Version 6.2, Schrödinger, LLC, New York, NY, 2014. Prime version 3.5.
[49] R.D. Cramer, D.E. Patterson, J.D. Bunce, Comparative molecular field analysis (CoMFA). 1. Effect of shape on binding of steroids to carrier proteins, J. Am. Chem. Soc. 110 (1988) 5959–5967.
[50] J.R. Savinainen, S.M. Saario, R. Niemi, T. Järvinen, J.T. Laitinen, An optimized approach to study endocannabinoid signaling: evidence against constitutive activity of rat brain adenosine A1 and cannabinoid CB1 receptors, Br. J. Pharmacol. 140 (2003) 1451–1459.
[51] J.R. Savinainen, T. Kokkola, O.M.H. Salo, A. Poso, T. Järvinen, J.T. Laitinen, Identification of WIN55212-3 as a competitive neutral antagonist of the human cannabinoid CB2 receptor, Br. J. Pharmacol. 145 (2005) 636–645.
[52] S.M. Saario, A. Poso, R.O. Juvonen, T. Järvinen, O.M. Salo-Ahen, Fatty acid amide hydrolase inhibitors from virtual screening of the endocannabinoid system, J. Med. Chem. 49 (15) (2006) 4650–4656.
[53] A. Minkkilä, S.M. Saario, H. Käsnänen, J. Leppänen, A. Poso, T. Nevalainen, Discovery of boronic acids as novel and potent inhibitors of fatty acid amide hydrolase, J. Med. Chem. 51 (2008) 7057–7060.
[54] D. Navia-Paldanius, J.R. Savinainen, J.T. Laitinen, Biochemical and pharmacological characterization of human α/β-hydrolase domain containing 6 (ABHD6) and 12 (ABHD12), J. Lipid. Res. 53 (2012) 2413–2424.